

# Disjunctive Benders Decomposition

Kaiwen Fang<sup>†‡</sup>

Inho Sin<sup>†‡</sup>

Geunyeong Byeon<sup>†§</sup>

## Abstract

We propose a novel enhancement to Benders decomposition (BD) that generates valid inequalities for the convex hull of the Benders reformulation, addressing a key limitation of conventional BD—its cuts are typically tight only for the continuous relaxation. Our method efficiently integrates disjunctive programming theory with BD, introducing a new routine that leverages existing cut-generating oracles for uncovering constraints required to construct valid inequalities for the convex hull. For mixed-binary linear programs, this approach eliminates the need to solve the master problem as a mixed-integer program. Additionally, we extend the a posteriori strengthening and lifting procedure for lift-and-project cuts into the BD framework, and present an approximate routine for generating lift-and-project cuts. Numerical results on large-scale instances show that our approach significantly reduces the number of branch-and-bound nodes required to reach the lower bound achieved by conventional BD, often by orders of magnitude.

*Key words:* Benders decomposition · disjunctive cuts · mixed-integer linear programs

## 1 Introduction

Benders decomposition (BD) is a widely used method for solving mixed-integer programming problems and has gained increasing attention for its effectiveness in tackling large-scale instances. Its versatility has led to numerous applications in areas such as power systems, transportation, and supply chain management (see [32] for a comprehensive review). This paper advances BD by addressing its inherent limitations through the integration of disjunctive programming theory [2, 3].

### 1.1 Problem statement

We focus on a mixed-integer linear programming (MILP) problem in the following form:

$$\begin{aligned} & \min_{x,y} c^\top x + d^\top y \\ & \text{s.t. } Ax + By \geq b, \\ & x \in \mathcal{X} := \{x \in [l_1, u_1] \times \cdots \times [l_{n_x}, u_{n_x}] : Dx \geq h, x_i \in \mathbb{Z}, \forall i \in \mathcal{I}\}, \end{aligned} \tag{MILP}$$

<sup>†</sup>School of Computing and Augmented Intelligence, Arizona State University, Tempe AZ, USA. Emails: {kfang11, inhosin, geunyeong.byeon}@asu.edu.

<sup>‡</sup>Equal contribution.

<sup>§</sup>Corresponding author.

where  $n_x$  is the dimension of  $x$ , and for each  $j \in [n_x] := \{1, \dots, n_x\}$ ,  $l_j$  and  $u_j$  denote the lower and upper bounds of  $x_j$ . The set  $\mathcal{I} \subseteq [n_x]$  represents the indices of  $x$  constrained to take integer values. Without loss of generality, we assume  $\mathcal{I} = \{1, \dots, \ell\}$ , where  $\ell = |\mathcal{I}|$ . All matrices and vectors, i.e.,  $A, B, D, c, d, b, h$ , are real and of appropriate dimensions. Fixing  $x$  simplifies the problem, as setting  $x = \hat{x}$  reduces the problem to a linear programming (LP) problem:

$$\min_y \{d^\top y : By \geq b - A\hat{x}\}. \quad (\text{sub}(\hat{x}))$$

Let  $\Pi$  denote the dual feasible region of  $\text{sub}(\hat{x})$ , that is  $\Pi = \{\pi \geq 0 : B^\top \pi = d\}$ . We make the following assumptions:

**Assumption 1.** (i) For each  $j \in \{1, \dots, n_x\}$ ,  $-\infty < l_j < u_j < \infty$ , i.e.,  $\mathcal{X}$  is compact.

(ii)  $\Pi \neq \emptyset$ .

**Remark 1.** Assumption 1(i) can be relaxed with some modifications to the derivations presented in this paper, but we impose it here for simplicity. Assumption 1(ii) is not restrictive, as  $\Pi = \emptyset$  would imply that  $\text{sub}(\hat{x})$  is infeasible or unbounded for any  $\hat{x} \in \mathbb{R}^{n_x}$ , rendering the problem pathological.

We define a value function  $f$  that maps  $\hat{x}$  to the optimal objective value of  $\text{sub}(\hat{x})$ . Its effective domain  $\text{dom}f := \{x \in \mathbb{R}^{n_x} : f(x) < \infty\}$  corresponds to the set of  $x$ 's for which  $\text{sub}(x)$  is feasible. Under Assumption 1(ii),  $\text{sub}(\hat{x})$  has strong dual for any  $\hat{x} \in \mathbb{R}^{n_x}$ . Thus, we have:

$$\begin{aligned} f(\hat{x}) &= \max_{\pi \in \Pi} (b - A\hat{x})^\top \pi && (\text{sub-dual}(\hat{x})) \\ &= \begin{cases} \max_{\hat{\pi} \in \mathcal{J}} (b - A\hat{x})^\top \hat{\pi} & \text{if } (b - A\hat{x})^\top \tilde{\pi} \leq 0, \forall \tilde{\pi} \in \mathcal{R} \\ \infty & \text{o.w.} \end{cases} \end{aligned}$$

where  $\mathcal{J}$  and  $\mathcal{R}$  respectively represent the set of all extreme points and extreme rays of  $\Pi$ . This implies  $\text{dom}f = \{x \in \mathbb{R}^{n_x} : 0 \geq \tilde{\pi}^\top (b - Ax), \forall \tilde{\pi} \in \mathcal{R}\}$  and  $\text{epi}f := \{(x, t) \in \mathbb{R}^{n_x+1} : t \geq f(x)\} = \{(x, t) \in \mathbb{R}^{n_x+1} : t \geq \hat{\pi}^\top (b - Ax), \forall \hat{\pi} \in \mathcal{J}\}$ , i.e.,  $\text{epi}f$  and  $\text{dom}f$  are polyhedral, and every facet of  $\text{epi}f$  (and  $\text{dom}f$ ) is associated with an extreme point (and an extreme ray) of the dual feasible region  $\Pi$ . We define a set

$$\mathcal{L} := \{(x, t) \in \mathbb{R}^{n_x+1} : (x, t) \in \text{epi}f, x \in \text{dom}f\}.$$

Using  $\mathcal{L}$ , (MILP) can be posed equivalently in the  $(x, t)$ -space, which is called *Benders reformulation*:

$$\min_{x \in \mathcal{X}, t \in \mathbb{R}} \{c^\top x + t : (x, t) \in \mathcal{L}\} = \min_{x \in \mathcal{X}, t \in \mathbb{R}} c^\top x + t \quad (1.1a)$$

$$\text{s.t. } t \geq \hat{\pi}^\top (b - Ax), \forall \hat{\pi} \in \mathcal{J}, \quad (1.1b)$$

$$0 \geq \tilde{\pi}^\top (b - Ax), \forall \tilde{\pi} \in \mathcal{R}. \quad (1.1c)$$

BD is an iterative algorithm for solving (1.1) which often involves exponential number of constraints for describing  $\mathcal{L}$ . It begins by replacing  $\mathcal{L}$  with a polyhedral relaxation in (1.1), forming what is known as the *master problem*, which generates candidate solutions. Given a candidate solution  $(\hat{x}, \hat{t})$ , an oracle verifies whether  $(\hat{x}, \hat{t}) \in \mathcal{L}$ . If not, the oracle constructs a hyperplane that separates  $(\hat{x}, \hat{t})$  from  $\mathcal{L}$  and adds it to the master problem, repeating this process iteratively.

The effectiveness of BD depends on two key factors: how the candidate solutions are generated and how the cut-generating oracle is designed. The candidate solutions can either be optimal solutions of the evolving master problem or a sequence of incumbent solutions identified during a branch-and-bound process. We refer to these approaches as BENDERSSEQ and BENDERSBNB, respectively. The BENDERSBNB method is particularly effective for large-scale problems, as it avoids solving the mixed-integer master problem at every iteration [19, 16, 32, 27].

The cut-generating oracle, another crucial component of BD, can take various forms. The simplest oracle solves **sub-dual** $(\hat{x})$ , computing  $f(\hat{x})$  and verifying whether the current solution  $(\hat{x}, \hat{t})$  violates the epigraph or domain conditions. If a violation is found, the oracle queries the solution or the unbounded ray of **sub-dual** $(\hat{x})$  to construct a violated inequality: either an *optimality cut* of the form (1.1b), separating the iterate from  $\text{epi } f$ , or a *feasibility cut* of the form (1.1c), separating it from  $\text{dom } f$ . A more advanced oracle may solve a modified subproblem to generate both optimality and feasibility cuts in a unified manner, often employing advanced cut-selection metrics [18, 22]. Alternatively, it may utilize a core point or analytical center to produce Pareto-optimal cuts [26, 30, 28, 34] or solve **sub-dual** $(x')$  for a perturbed point  $x'$ , often obtained as a convex combination of  $\hat{x}$  and a reference point [7, 16]. Recently, artificial intelligence-informed oracles have been developed to identify effective Benders cuts from the  $n$ -best candidates generated by the aforementioned oracles [23, 15]. All these oracle variants generate hyperplanes that separate the solution from  $\mathcal{L}$ , as illustrated in Figure 1a. Throughout this paper, we refer to these oracles as **TYPICALORACLE**.

However, BD has an inherent limitation: the cuts generated by a **TYPICALORACLE** are *at best tight with respect to  $\mathcal{L}$* . In other words, the oracle generating these cuts does not account for the integrality constraints on  $x$ . Although such oracles have shown efficiency in various applications, their performance can degrade significantly when the integrality gap in (1.1) is large—that is, when the convex hull of  $(\mathcal{X} \times \mathbb{R}) \cap \mathcal{L}$  is much smaller than  $\mathcal{L}$ . This limitation impacts the efficiency of both BENDERSSEQ and BENDERSBNB and we conjecture that it is a major contributor to the commonly observed tail-off convergence of BD [12], where substantial progress is often made during the initial iterations, but then the algorithm slows considerably thereafter, achieving only minimal

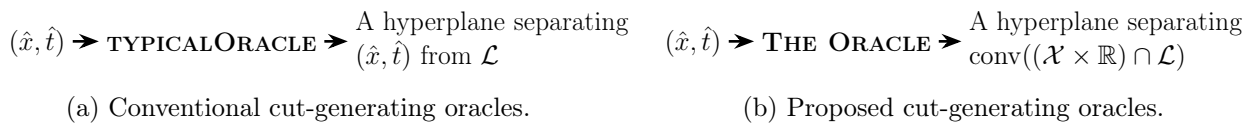
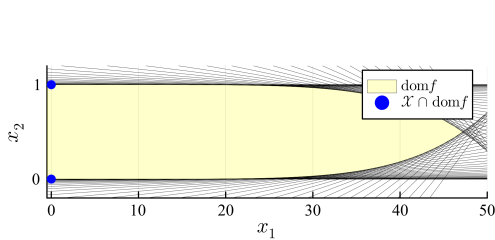
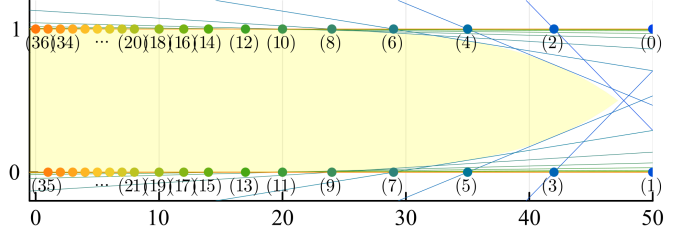


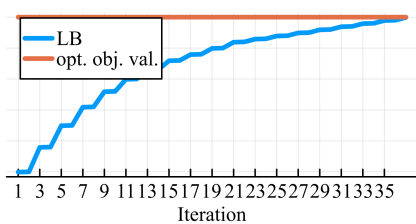
Figure 1: Comparison between the proposed approach and conventional methods.



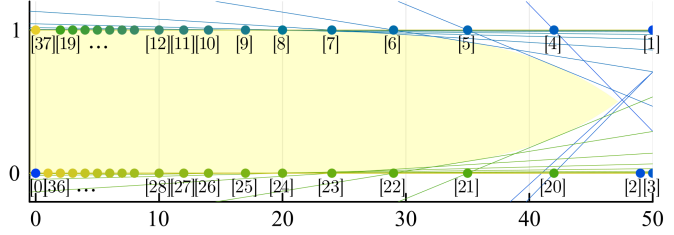
(a) Instance visualization.



(b) Iterates  $\{x^{(k)}\}$  and cuts produced by BENDERSSSEQ; colors associate  $x^{(k)}$  and the cuts.



(c) Tail-off convergence.



(d) Candidate incumbent solutions  $\{\hat{x}^{[k]}\}$  and cuts produced by BENDERSSBNB.

Figure 2: Visualization of BD’s behavior; horizontal (or vertical) axes for  $x_1$  (or  $x_2$ ).

reductions in the optimality gap over many iterations. This behavior is illustrated in the following example, which motivates the development of an oracle capable of generating cuts that are valid for the convex hull of  $(\mathcal{X} \times \mathbb{R}) \cap \mathcal{L}$ , as defined in Figure 1b.

## 1.2 Motivating example

We illustrate from a simple example that even with a state-of-the-art implementation, BD may need to enumerate a substantial portion of the discrete set  $\mathcal{X}$  before reaching an optimal solution.

Consider an instance of (1.1) with  $\mathcal{X} = \{0, 1, \dots, 50\} \times \{0, 1\}$  and  $c = [-2; -1]$ . Assume  $f(x) = 0$  for  $x \in \text{dom } f$ , resulting in the Benders reformulation:  $\min\{c^\top x : x \in \mathcal{X} \cap \text{dom } f\}$ . As depicted in Figure 2a,  $\text{dom } f$  is characterized by hyperplanes with gradually changing slopes so that only two points (marked in blue) are feasible, i.e., in  $\mathcal{X} \cap \text{dom } f$ . The optimal solution can be easily identified as  $(0, 1)$ .

Figures 2b and 2d depict the iterates  $\{x^{(k)}\}$  and the incumbent solutions  $\{\hat{x}^{[k]}\}$  generated by BENDERSSSEQ and BENDERSSBNB, respectively, both equipped with an advanced TYPICALORACLE proposed in [18] and implemented via the Julia-CPLEX interface. Even in this simple example, both methods enumerate more than a quarter of  $\mathcal{X}$ . Figure 2b highlights the trajectory of BENDERSSSEQ, which zigzags across more than a quarter of  $\mathcal{X}$ , resulting in the tailing-off convergence behavior depicted in Figure 2c. Meanwhile, although BENDERSSBNB may identify a high-quality incumbent solution early on, as shown in Figure 2d, proving its optimality requires a substantial number of cuts, resulting in a final search tree with 16 nodes.

It is important to mention that this example is not considered pathological. For example, when dealing with bilevel programs involving convex followers, the Benders reformulations of these bilevel programs exhibit a similar pattern due to the incorporation of large coefficients to render the follower’s optimality condition convex. These coefficients lead the Benders cuts to remove just one potential solution point during each iteration, a phenomenon that was observed in [12].

If cutting planes are generated for the convex hull of  $\mathcal{X} \cap \text{dom } f$ , instead of  $\text{dom } f$ , the algorithm would terminate right away or in a few iterations. This example highlights why the simple in-out method [7, 16], which separates  $\lambda x^{(k)} + (1 - \lambda)\hat{x}^0$  for some  $\lambda \in [0, 1]$  and a core point  $\hat{x}^0$ , instead of  $x^{(k)}$ , is often found to be effective [27]. Nevertheless, this example suggests that the performance of the in-out method is limited and can vary significantly depending on the choice of  $\hat{x}^0$  and  $\lambda$ , which are challenging to determine a priori.

### 1.3 Related literature

Generating cuts for the convex hull of  $(\mathcal{X} \times \mathbb{R}) \cap \mathcal{L}$  can yield significantly stronger cuts, reducing the total number of iterations in BENDERSSEQ or shrinking the branch-and-bound tree in BENDERSBNB. Only recently have attempts been made to incorporate the integrality of  $x$  into Benders cut generation to make the cuts stronger [11, 10, 35, 31]. In [35, 31], the authors introduced binary variables to the subproblems to generate stronger Lagrangian-based cuts. In [11], a mixed-rounding procedure was applied to already-generated Benders cuts to further strengthen them. Another relevant work, [10], introduced split cuts, termed project-and-cut split cuts, which are derived from a cut-generating problem formulated based on the original formulation (MILP). Since the resultant cut-generating linear program can become enormous, they experimented with adding split cuts for the current master problem—i.e., for the convex hull of  $(\mathcal{X} \times \mathbb{R}) \cap \widehat{\mathcal{L}}$ , where  $\widehat{\mathcal{L}}$  is an outer approximation of  $\mathcal{L}$ —as well as solving the proposed cut-generating problem separately for each scenario. They also proposed another method, termed cut-and-project split cuts, which incorporate valid constraints for the Lagrangian subproblems to the Benders subproblems, akin to cuts proposed for solving stochastic integer programming [33, 20]. We provide a detailed comparison of the proposed approach with these existing methods in Section 4.

### 1.4 Contributions

We propose a novel approach to enhancing BD by incorporating the generation of valid inequalities for the convex hull of the Benders reformulation. This addresses a key limitation of conventional BD, which typically generates cuts that can be at best tight with respect to the continuous relaxation. Our main contributions are summarized as follows:

- *A general and scalable framework for generating disjunctive cuts for the Benders reformulation (i.e., (1.1)).* We develop a scalable routine that leverages existing cut-generating oracles to identify unknown constraints essential for generating disjunctive cuts. When fully executed, the routine constructs a supporting hyperplane for a set lying between the convex hull and the

continuous relaxation. Notably, even if the routine terminates early, it still produces a valid inequality that cuts off part of the continuous relaxation, ensuring computational efficiency and practical applicability. This routine offers advantages over related approaches, particularly for large-scale problems, as it neither introduces integer variables into the subproblem nor operates directly on the original formulation (MILP) (see Section 4 for details).

- *Advancements for mixed-binary linear programs.* For mixed-binary linear programs, we show that a specialized integration of the proposed routine within BD eliminates the need to solve the master problem as a mixed-integer program. Additionally, we extend the a posteriori strengthening and lifting procedure for lift-and-project cuts—an important class of disjunctive cuts for mixed-binary linear programs—into the BD framework. This extension provides a simple yet effective method for enhancing lift-and-project cuts produced by the proposed routine. Furthermore, it motivates the development of an approximate routine that efficiently identifies a lift-and-project cut whenever a violation exists.
- *Numerical experiments.* We conduct numerical experiments on large-scale instances of the uncapacitated facility location problem and the stochastic network interdiction problem, demonstrating the effectiveness of disjunctive cuts in improving the node efficiency of BENDERSBNB—measured as the rate of lower bound improvement relative to the number of nodes explored. The proposed approach successfully solves instances that neither an off-the-shelf solver nor a state-of-the-art Benders implementation can solve, and it reduces final tree sizes by up to an order of magnitude on relatively difficult instances. Even in cases where no method reaches optimality, the approach alleviates the tail-off behavior commonly observed in classical BD.

## 1.5 Notation and Organization of the Paper

In this paper, we use the following notation:  $\mathbb{Z}$  and  $\mathbb{R}$  respectively denote the set of integers and real numbers. For any set  $\mathcal{S} \in \{\mathbb{Z}, \mathbb{R}\}$ , the notation  $\mathcal{S}_{\geq 0}$  (or  $\mathcal{S}_{> 0}$ ) refers to the set of elements in  $\mathcal{S}$  that are greater than or equal to (or strictly greater than) zero. The set  $[n]$  represents the set  $\{1, 2, \dots, n\}$ . The boldfaced  $\mathbf{0}$  is a vector of zeros. The convex hull of a set  $\mathcal{S}$  is denoted by  $\text{conv}(\mathcal{S})$ , and the notation  $\|\cdot\|_p$  represents the  $l_p$ -norm for some  $p \in [1, \infty]$ , and  $q$  is such that  $1/p + 1/q = 1$ . The vector  $e_j$  denotes the  $j$ -th unit vector. For a vector  $v$  and a scalar  $a$ ,  $(v, a)$  denotes their concatenation, and  $\text{Proj}_x(\mathcal{S})$  refers to the orthogonal projection of a set  $\mathcal{S}$  onto the  $x$ -space.

This paper is organized as follows: Section 2 presents the proposed approach, starting with the formal definition of the disjunction in the Benders reformulation in Section 2.1, followed by the development of a cut-generating problem in Section 2.2, an oracle for solving this problem in Section 2.3, and the disjunctive Benders decomposition incorporating the proposed oracle in Section 2.4. Section 3 discusses further advancements for mixed-binary linear programs. Section 4 compares the proposed approach with relevant literature. Section 5 evaluates the effectiveness of the disjunctive Benders decomposition through experimental studies. Finally, Section 6 concludes the paper. Omitted proofs are provided in Appendix A.

## 2 Proposed approach: disjunctive Benders decomposition

Since Balas's seminal work [1], disjunctive cuts have been extensively used to solve mixed-integer programs in both linear and nonlinear convex settings [3]. Notably, disjunctive cuts—particularly split cuts, which are derived from two-term disjunctions—subsume several prominent classes of cutting planes, including Chvátal-Gomory cuts, Gomory Mixed-Integer cuts, and Mixed-Integer Rounding cuts [13]. Disjunctions are useful for conveying integrality information in the cut-generation process. In this section, we propose a method to strengthen Benders cuts by leveraging disjunctions.

### 2.1 Disjunction of the Benders reformulation

An integral vector  $(\phi, \phi_0) \in \mathbb{Z}^{n_x+1}$  is called a *split* for (1.1) if  $\phi_j = 0$  for all  $j \in [n_x] \setminus \mathcal{I}$ , ensuring that  $\phi^\top x \in \mathbb{Z}$  for any  $x \in \mathcal{X}$ . By construction, the disjunction  $\phi^\top x \leq \phi_0 \vee \phi^\top x \geq \phi_0 + 1$  does not exclude any point in  $\mathcal{X}$ . Using a split  $(\phi, \phi_0)$ , a union of polyhedra  $\mathcal{P}^{(\phi, \phi_0)} := \mathcal{P}_1^{(\phi, \phi_0)} \cup \mathcal{P}_2^{(\phi, \phi_0)}$  can be constructed, where

$$\mathcal{P}_1^{(\phi, \phi_0)} := \mathcal{P} \cap \{(x, t) : \phi^\top x \geq \phi_0 + 1\}, \quad \mathcal{P}_2^{(\phi, \phi_0)} := \mathcal{P} \cap \{(x, t) : \phi^\top x \leq \phi_0\},$$

and  $\mathcal{P}$  denotes the continuous relaxation of the feasible region of (1.1), i.e.,  $\mathcal{P} = (\mathcal{X}_{LP} \times \mathbb{R}) \cap \mathcal{L}$  where  $\mathcal{X}_{LP} = \{x \in \mathbb{R}^{n_x} : l \leq x \leq u, Dx \geq h\}$ . More specifically,

$$\begin{array}{ll} \mathcal{P}_1^{(\phi, \phi_0)} : & \mathcal{P}_2^{(\phi, \phi_0)} : \\ (\lambda_{\hat{\pi}}^1) & t \geq \hat{\pi}^\top (b - Ax), \quad \forall \hat{\pi} \in \mathcal{J}, \\ (\mu_{\tilde{\pi}}^1) & 0 \geq \tilde{\pi}^\top (b - Ax), \quad \forall \tilde{\pi} \in \mathcal{R}, \\ (\theta^1) & Dx \geq h, \\ (\sigma^1) & \phi^\top x \geq \phi_0 + 1, \\ (\eta^1) & -x \geq -u, \\ (\delta^1) & x \geq l \end{array} \quad \bigvee \quad \begin{array}{ll} \mathcal{P}_1^{(\phi, \phi_0)} : & \mathcal{P}_2^{(\phi, \phi_0)} : \\ (\lambda_{\hat{\pi}}^2) & t \geq \hat{\pi}^\top (b - Ax), \quad \forall \hat{\pi} \in \mathcal{J}, \\ (\mu_{\tilde{\pi}}^2) & 0 \geq \tilde{\pi}^\top (b - Ax), \quad \forall \tilde{\pi} \in \mathcal{R}, \\ (\theta^2) & Dx \geq h, \\ (\sigma^2) & -\phi^\top x \geq -\phi_0, \\ (\eta^2) & -x \geq -u, \\ (\delta^2) & x \geq l \end{array}$$

where the variables in parentheses denote the Farkas multipliers associated with each constraint.

Note that  $\text{conv}((\mathcal{X} \times \mathbb{R}) \cap \mathcal{L}) \subseteq \text{conv}(\mathcal{P}^{(\phi, \phi_0)}) \subseteq \mathcal{P} \subseteq \mathcal{L}$ , as the split conveys partial integrality information. It is known that the second inclusion is strict when at least one vertex  $x'$  of  $\mathcal{P}$  satisfies  $\phi_0 < \phi^\top x' < \phi_0 + 1$  (see, e.g., [13, Proposition 5.2]). Moreover, when all integer variables are binaries (i.e.,  $[l_j, u_j] = [0, 1]$  for all  $j \in \mathcal{I} = \{1, \dots, \ell\}$ ), the following holds from the sequential convexification theorem [2]:

$$\text{conv}((\mathcal{X} \times \mathbb{R}) \cap \mathcal{L}) = \text{conv}(\mathcal{P}^{(e_\ell, 0)} \cap \text{conv}(\dots \cap \text{conv}(\mathcal{P}^{(e_2, 0)} \cap \text{conv}(\mathcal{P}^{(e_1, 0)})) \dots)).$$

This implies that  $\text{conv}(\mathcal{X} \times \mathbb{R}) \cap \mathcal{L}$  can be obtained by iteratively adding valid inequalities for simple disjunctive systems,  $\text{conv}(\mathcal{P}^{(e_j, 0)})$  for  $j \in \mathcal{I}$ , in a specialized augmented manner [2]. We propose a routine that generates tight valid inequalities for  $\text{conv}(\mathcal{P}^{(\phi, \phi_0)})$ .

## 2.2 Cut-generating linear program

Typically, disjunctive cuts are generated by solving the so-called cut-generating linear program (CGLP), originally introduced by Balas [1]. The CGLP utilizes Farkas multipliers to characterize valid inequalities for  $\text{conv}(\mathcal{P}^{(\phi, \phi_0)})$  in an extended space, with its objective function and a normalization constraint determining the specific inequality to generate.

### 2.2.1 Valid inequalities for $\text{conv}(\mathcal{P}^{(\phi, \phi_0)})$

Assume both  $\mathcal{P}_1^{(\phi, \phi_0)}$  and  $\mathcal{P}_2^{(\phi, \phi_0)}$  are nonempty. An inequality  $\hat{\gamma}_0 - \hat{\gamma}_x^\top x - \hat{\gamma}_t t \leq 0$  is a valid inequality for both  $\mathcal{P}_1^{(\phi, \phi_0)}$  and  $\mathcal{P}_2^{(\phi, \phi_0)}$ , i.e., for  $\mathcal{P}_1^{(\phi, \phi_0)} \cup \mathcal{P}_2^{(\phi, \phi_0)}$ , if and only if  $(\hat{\gamma}_0, \hat{\gamma}_x, \hat{\gamma}_t)$  meets the following constraints (see, e.g., [3, Theorems 1.2]):

$$(\kappa_t) \quad \gamma_t = \sum_{\hat{\pi} \in \mathcal{J}} \lambda_{\hat{\pi}}^1, \quad (2.1a)$$

$$(\nu_t) \quad \gamma_t = \sum_{\hat{\pi} \in \mathcal{J}} \lambda_{\hat{\pi}}^2, \quad (2.1b)$$

$$(\kappa_x) \quad \gamma_x = \sum_{\tilde{\pi} \in \mathcal{R}} \mu_{\tilde{\pi}}^1 A^\top \tilde{\pi} + \sum_{\hat{\pi} \in \mathcal{J}} \lambda_{\hat{\pi}}^1 A^\top \hat{\pi} + D^\top \theta^1 + \phi^\top \sigma^1 - \eta^1 + \delta^1, \quad (2.1c)$$

$$(\nu_x) \quad \gamma_x = \sum_{\tilde{\pi} \in \mathcal{R}} \mu_{\tilde{\pi}}^2 A^\top \tilde{\pi} + \sum_{\hat{\pi} \in \mathcal{J}} \lambda_{\hat{\pi}}^2 A^\top \hat{\pi} + D^\top \theta^2 - \phi^\top \sigma^2 - \eta^2 + \delta^2, \quad (2.1d)$$

$$(\kappa_0) \quad \gamma_0 \leq \sum_{\tilde{\pi} \in \mathcal{R}} \mu_{\tilde{\pi}}^1 \tilde{\pi}^\top b + \sum_{\hat{\pi} \in \mathcal{J}} \lambda_{\hat{\pi}}^1 \hat{\pi}^\top b + h^\top \theta^1 + (\phi_0 + 1) \sigma^1 - u^\top \eta^1 + l^\top \delta^1, \quad (2.1e)$$

$$(\nu_0) \quad \gamma_0 \leq \sum_{\tilde{\pi} \in \mathcal{R}} \mu_{\tilde{\pi}}^2 \tilde{\pi}^\top b + \sum_{\hat{\pi} \in \mathcal{J}} \lambda_{\hat{\pi}}^2 \hat{\pi}^\top b + h^\top \theta^2 - \phi_0 \sigma^2 - u^\top \eta^2 + l^\top \delta^2, \quad (2.1f)$$

$$(\lambda_{\hat{\pi}}^r)_{\hat{\pi} \in \mathcal{J}}, (\mu_{\tilde{\pi}}^r)_{\tilde{\pi} \in \mathcal{R}}, \theta^r, \sigma^r, \eta^r, \delta^r \geq 0, \quad r = 1, 2, \quad (2.1g)$$

where the variables in parentheses are the associated dual variables. We let  $\gamma := (\gamma_0, \gamma_x, \gamma_t)$  and let  $\chi := ((\lambda_{\hat{\pi}}^r)_{\hat{\pi} \in \mathcal{J}}, (\mu_{\tilde{\pi}}^r)_{\tilde{\pi} \in \mathcal{R}}, \theta^r, \sigma^r, \eta^r, \delta^r)_{r=1,2}$ . Let  $\Gamma$  denote the projection of the region defined by (2.1) onto the  $\gamma$ -space, i.e.,

$$\Gamma := \{\gamma : \exists \chi \text{ s.t. } (\gamma, \chi) \text{ meets (2.1)}\}. \quad (2.2)$$

### 2.2.2 Normalization constraints

Based on the characterization of valid inequalities in Section 2.2.1, when both  $\mathcal{P}_1^{(\phi, \phi_0)}$  and  $\mathcal{P}_2^{(\phi, \phi_0)}$  are nonempty, one may want to verify whether  $(\hat{x}, \hat{t})$  lies within  $\text{conv}(\mathcal{P}^{(\phi, \phi_0)})$  and, if it does not, separate  $(\hat{x}, \hat{t})$  from  $\text{conv}(\mathcal{P}^{(\phi, \phi_0)})$  by maximizing the violation as follows:

$$\max\{\gamma_0 - \gamma_x^\top \hat{x} - \gamma_t \hat{t} : \gamma \in \Gamma\}. \quad (2.3)$$

Since the feasible region  $\Gamma$  is conic (i.e.,  $\alpha\gamma \in \Gamma$  for any  $\alpha \in \mathbb{R}_{\geq 0}$  and  $\gamma \in \Gamma$ ), Problem (2.3) becomes unbounded whenever  $(\hat{x}, \hat{t}) \notin \text{conv}(\mathcal{P}^{(\phi, \phi_0)})$ . To address this issue, it is necessary to impose a

normalization constraint on (2.3) to ensure boundedness and generate meaningful inequalities.

The choice of normalization constraint plays a critical role in generating effective disjunctive cuts, as widely discussed in the literature [17, 25]. A commonly used normalization approach is referred to as standard normalization, which imposes  $\|\chi\|_1 = 1$ . However, as noted in [17], this method is susceptible to issues such as redundancy in constraints and sensitivity to constraint scaling. Specifically, even a weak cut may appear to be the most violated one in the presence of redundant constraints or when constraints are improperly scaled; a cut generated with standard normalization is not necessarily a supporting hyperplane to  $\text{conv}(\mathcal{P}^{(\phi, \phi_0)})$ .

This issue is particularly problematic in the context of BD, where numerous constraints may remain unknown, making it challenging to manage redundancy as the problem is augmented with disjunctive cuts. Additionally, feasibility cuts, defined by rays, can be arbitrarily scaled.

Therefore, we advocate for the use of  $\gamma$ -normalization, as it can circumvent scaling and redundancy issues completely by finding a valid inequality whose distance from the separation point  $(\hat{x}, \hat{t})$  is maximized in a  $l_p$ -norm sense for some  $p \in [1, \infty]$ , ensuring the generation of a supporting hyperplane to  $\text{conv}(\mathcal{P}^{(\phi, \phi_0)})$ , as will be elaborated later.

Formally, the  $\|\cdot\|_p$ -based distance  $d_p(\hat{\gamma}; \hat{x}, \hat{t})$  between  $(\hat{x}, \hat{t})$  and a halfspace  $\hat{\gamma}_x^\top x + \hat{\gamma}_t t \geq \hat{\gamma}_0$  is defined as:

$$\begin{aligned} d_p(\hat{\gamma}; \hat{x}, \hat{t}) &:= \min_{(x, t) \in \mathbb{R}^{n_x+1}} \|(x, t) - (\hat{x}, \hat{t})\|_p : \hat{\gamma}_x^\top x + \hat{\gamma}_t t \geq \hat{\gamma}_0 \\ &= \max_{\iota \geq 0} \min_{(x, t) \in \mathbb{R}^{n_x+1}} \|(x, t) - (\hat{x}, \hat{t})\|_p + \iota(\hat{\gamma}_0 - \hat{\gamma}_x^\top x - \hat{\gamma}_t t) \\ &= \max_{\iota \geq 0} \min_{(x', t') \in \mathbb{R}^{n_x+1}} \|(x', t')\|_p + \iota(\hat{\gamma}_0 - \hat{\gamma}_x^\top(\hat{x} + x') - \hat{\gamma}_t(\hat{t} + t')) \\ &= \max_{\iota \geq 0} \iota(\hat{\gamma}_0 - \hat{\gamma}_x^\top \hat{x} - \hat{\gamma}_t \hat{t}) - \max_{(x', t') \in \mathbb{R}^{n_x+1}} \iota(\hat{\gamma}_x^\top x' + \hat{\gamma}_t t') - \|(x', t')\|_p \\ &= \max_{\iota \geq 0} \iota(\hat{\gamma}_0 - \hat{\gamma}_x^\top \hat{x} - \hat{\gamma}_t \hat{t}) : \|\iota(\hat{\gamma}_x, \hat{\gamma}_t)\|_q \leq 1, \end{aligned}$$

where the second equality follows from strong duality, which is guaranteed by the weak version of Slater's condition. The third equality arises from a change of variables using  $(x', t') = (x, t) - (\hat{x}, \hat{t})$ , and the last equality is derived from the conjugate of the norm function, where  $q$  denotes the Hölder constant corresponding to the  $l_p$ -norm, satisfying  $\frac{1}{p} + \frac{1}{q} = 1$ .

Therefore, the *deepest* disjunctive cut can be generated by solving the following CGLP:

$$\begin{aligned} \max\{d_p(\gamma; \hat{x}, \hat{t}) : \gamma \in \Gamma\} &= \max_{\iota \geq 0, \gamma} \{\iota(\gamma_0 - \gamma_x^\top \hat{x} - \gamma_t \hat{t}) : \|\iota(\gamma_x, \gamma_t)\|_q \leq 1, \gamma \in \Gamma\} \\ &= \max_{\gamma} \{\gamma_0 - \gamma_x^\top \hat{x} - \gamma_t \hat{t} : \|\gamma\|_q \leq 1, \gamma \in \Gamma\}, \end{aligned} \quad (\text{CGLP})$$

where the second equality holds because  $\Gamma$  is conic. Specifically, for any feasible  $(\iota, \gamma)$  in the first formulation, the scaled variable  $\gamma' = \iota\gamma$  is feasible in the second formulation with the same objective value. Conversely, for any feasible  $\gamma$  in the second formulation, the pair  $(\iota', \gamma') = (1, \gamma)$  is feasible in the first formulation with the same objective value. Additionally, when  $p \in \{1, \infty\}$ , the

normalization constraint  $\|(\gamma_x, \gamma_t)\|_q \leq 1$  can be expressed using  $O(n_x)$  linear inequalities. Therefore, for  $p \in \{1, \infty\}$ , the problem is indeed a linear program.

**Remark 2.** Problem (CGLP) shares some similarities with the deepest Benders cut generation procedure proposed in [22], as both aim to identify the deepest cut for a set based on a specified distance metric. However, they differ in the set for which the deepest cut is generated. In [22], the deepest cut is generated with respect to  $\mathcal{L}$ . In contrast, (CGLP) concerns the set  $\text{conv}(\mathcal{P}^{(\phi, \phi_0)}) \subseteq \mathcal{L}$ , resulting in a potentially much stronger cut. This inclusion is strict whenever there exists at least one extreme point of  $\mathcal{L}$  that violates the disjunction constructed by the split  $(\phi, \phi_0)$ . Furthermore,  $\text{conv}(\mathcal{P}^{(\phi, \phi_0)})$  can be significantly smaller than  $\mathcal{L}$  in the presence of a substantial integrality gap.

### 2.2.3 The dual of (CGLP)

Note that directly solving (CGLP) is impractical, as it typically involves an exponential number of variables associated with  $\mathcal{J}$  and  $\mathcal{R}$ . In this section, we present key properties and insights from the dual of (CGLP), which inspire the design of a practical oracle for generating the deepest disjunctive cuts for (1.1). The dual of (CGLP), using the dual variables defined in the parentheses in (2.1), is given below and is denoted as (DCGLP):

$$\begin{aligned}
& \min \tau && (\text{DCGLP.a}) \\
\text{s.t. } & (\kappa_x, \kappa_t, \kappa_0) \in \mathcal{L}^\#, && (\text{DCGLP.b}) \\
& (\kappa_x, \kappa_0) \in \mathcal{X}_{LP}^\#, && (\text{DCGLP.c}) \\
& \phi^\top \kappa_x \geq (\phi_0 + 1)\kappa_0, && (\text{DCGLP.d}) \\
& (\nu_x, \nu_t, \nu_0) \in \mathcal{L}^\#, && (\text{DCGLP.e}) \\
& (\nu_x, \nu_0) \in \mathcal{X}_{LP}^\#, && (\text{DCGLP.f}) \\
& -\phi^\top \nu_x \geq -\phi_0 \nu_0, && (\text{DCGLP.g}) \\
& \kappa_0 \geq 0, \nu_0 \geq 0, && (\text{DCGLP.h}) \\
& (\gamma_0) \quad \kappa_0 + \nu_0 = 1, && (\text{DCGLP.i}) \\
& (\gamma_x) \quad s_x = \kappa_x + \nu_x - \hat{x}, && (\text{DCGLP.j}) \\
& (\gamma_t) \quad s_t = \kappa_t + \nu_t - \hat{t}, && (\text{DCGLP.k}) \\
& \tau \geq \|(s_x, s_t)\|_p. && (\text{DCGLP.l})
\end{aligned}$$

Here,  $\mathcal{Q}^\#$  denotes a raised representation of a polyhedron  $\mathcal{Q} := \{u \in \mathbb{R}^n : Au \leq b\}$  in a space of one higher dimension, obtained by scaling all the right-hand side expressions with a new nonnegative variable; specifically,  $\mathcal{Q}^\# = \{(u, v) \in \mathbb{R}^n \times \mathbb{R}_{\geq 0} : Au \leq bv\}$ . For instance,  $\mathcal{L}^\# = \{(x, t, z) \in \mathbb{R}^{n_x+1} \times \mathbb{R}_{\geq 0} : t \geq \hat{\pi}^\top (bz - Ax), \forall \hat{\pi} \in \mathcal{J}, 0 \geq \tilde{\pi}^\top (bz - Ax), \forall \tilde{\pi} \in \mathcal{R}\}$  and  $\mathcal{X}_{LP}^\# = \{(x, z) \in \mathbb{R}^{n_x} \times \mathbb{R}_{\geq 0} : Dx \geq hz, x \geq lz, -x \geq -uz\}$ . Note that  $\mathcal{Q}$  is an image of  $\mathcal{Q}^\# \cap \{(u, v) : v > 0\}$  under the perspective mapping.

**Lemma 1.** (CGLP) and (DCGLP) enjoy strong duality, and (DCGLP) is equivalent to the following projection problem:

$$\min \| (x, t) - (\hat{x}, \hat{t}) \|_p : (x, t) \in \text{conv}(\mathcal{P}^{(\phi, \phi_0)}), \quad (2.4)$$

which computes the projection of  $(\hat{x}, \hat{t})$  onto the convex set  $\text{conv}(\mathcal{P}^{(\phi, \phi_0)})$  in the  $l_p$ -norm sense, i.e., it identifies the point in  $\text{conv}(\mathcal{P}^{(\phi, \phi_0)})$  that is closest to  $(\hat{x}, \hat{t})$  with respect to the  $\| \cdot \|_p$ -norm.

Lemma 1 is key to establish that (DCGLP) is well-defined in the sense that it attains a finite optimum whenever  $\mathcal{P}^{(\phi, \phi_0)} \neq \emptyset$ , i.e., when (MILP) is feasible; otherwise, it correctly identifies infeasibility. Furthermore, it implies that the generated cut serves as a supporting hyperplane to  $\text{conv}(\mathcal{P}^{(\phi, \phi_0)})$ :

**Proposition 1.** *If (MILP) is feasible, then (DCGLP) attains a finite, nonnegative optimal objective value for any given split  $(\phi, \phi_0)$ ; otherwise, (DCGLP) is infeasible. Moreover, if (DCGLP) has a positive optimal objective value, then the valid inequality  $\hat{\gamma}_0 - \hat{\gamma}_x^\top x - \hat{\gamma}_t^\top t \leq 0$ , where  $\hat{\gamma}$  is the optimal dual solution associated with (DCGLP.i)–(DCGLP.k), defines a supporting hyperplane to  $\text{conv}(\mathcal{P}^{(\phi, \phi_0)})$ . Specifically, there exists a point  $(x', t') \in \text{conv}(\mathcal{P}^{(\phi, \phi_0)})$  such that  $\hat{\gamma}_x^\top x' + \hat{\gamma}_t^\top t' = \hat{\gamma}_0$ . If the optimal objective value is zero, then  $(\hat{x}, \hat{t}) \in \text{conv}(\mathcal{P}^{(\phi, \phi_0)})$ .*

**Remark 3** (Interpretation of the optimal solution of (DCGLP)). *The proofs of Lemma 1 and Proposition 1 offer an insightful interpretation of the optimal solution of (DCGLP). Let  $(\hat{\kappa}, \hat{\nu}, \hat{s}, \hat{t})$  (and  $\hat{\gamma}$ ) be the optimal primal (and dual) solution of (DCGLP). If both  $\hat{\kappa}_0$  and  $\hat{\nu}_0$  are positive, then  $(\hat{\kappa}_x + \hat{\nu}_x, \hat{\kappa}_t + \hat{\nu}_t)$  corresponds to the projection of  $(\hat{x}, \hat{t})$  onto  $\text{conv}(\mathcal{P}^{(\phi, \phi_0)})$ . In this case,  $(\hat{\kappa}_x/\hat{\kappa}_0, \hat{\kappa}_t/\hat{\kappa}_0) \in \mathcal{P}_1^{(\phi, \phi_0)}$  and  $(\hat{\nu}_x/\hat{\nu}_0, \hat{\nu}_t/\hat{\nu}_0) \in \mathcal{P}_2^{(\phi, \phi_0)}$ , and the projection point is a convex combination of these two points. If  $\hat{\nu}_0 = 0$  (or  $\hat{\kappa}_0 = 0$ ), then the projection point lies in  $\mathcal{P}_1^{(\phi, \phi_0)}$  at  $(\hat{\kappa}_x, \hat{\kappa}_t)$  (or in  $\mathcal{P}_2^{(\phi, \phi_0)}$  at  $(\hat{\nu}_x, \hat{\nu}_t)$ ). Furthermore, the projection point  $(\hat{\kappa}_x + \hat{\nu}_x, \hat{\kappa}_t + \hat{\nu}_t)$  is the intersection of the valid inequality  $\hat{\gamma}_x^\top x + \hat{\gamma}_t^\top t \geq \hat{\gamma}_0$  with  $\text{conv}(\mathcal{P}^{(\phi, \phi_0)})$ .*

## 2.3 THE ORACLE

Lemma 1, Proposition 1, and Remark 3 offer valuable insights and properties of (DCGLP). Building on these results, we propose an oracle for generating disjunctive cuts for the Benders reformulation (1.1), which we refer to as *disjunctive Benders cuts*. Within this oracle, (DCGLP) is solved via a cutting plane algorithm, and then the simple retrieval of (optimal) dual solutions associated with (DCGLP.i)–(DCGLP.k) generates (the deepest) disjunctive Benders cuts.

Note that (DCGLP) involves  $\mathcal{L}^\#$ , which is often defined by an exponential number of constraints associated with  $\mathcal{J}$  and  $\mathcal{R}$ . However,  $\mathcal{L}^\#$  has a key property, outlined in the following proposition, which allows us to generate separating hyperplanes of  $\mathcal{L}^\#$  using typical Benders oracles (see Figure 1a for the definition of typical Benders oracles), without the need to have all the constraints upfront:

**Proposition 2.** *Let  $(\hat{\omega}_x, \hat{\omega}_t, \hat{\omega}_0) \in \mathbb{R}^{n_x+1} \times \mathbb{R}_{>0}$ . Suppose there exists a hyperplane of the form  $\alpha_x^\top x + \alpha_t^\top t \geq \alpha_0$  that separates  $(x', t') := (\hat{\omega}_x/\hat{\omega}_0, \hat{\omega}_t/\hat{\omega}_0)$  from  $\mathcal{L}$ . Then, the hyperplane  $\alpha_x^\top \omega_x +$*

$\alpha_t \omega_t \geq \alpha_0 \omega_0$  separates  $(\hat{\omega}_x, \hat{\omega}_t, \hat{\omega}_0)$  from  $\mathcal{L}^\#$ . Conversely, if  $(x', t') \in \mathcal{L}$ , meaning no such separating hyperplane exists, then  $(\hat{\omega}_x, \hat{\omega}_t, \hat{\omega}_0) \in \mathcal{L}^\#$ .

Proposition 2 motivates Routine 1 for generating disjunctive Benders cuts. The routine iteratively refines a relaxation,  $\mathbf{R}$ , of (DCGLP), starting with an initial approximation of  $\mathcal{L}$  that includes at least one optimality cut or a trivial lower bound on  $t$  (e.g.,  $t \geq -10^{99}$ ). This guarantees that the relaxation of  $\mathcal{L}^\#$  contains at least one constraint of the form  $t \geq \hat{\pi}^\top (bz - Ax)$  for some  $\hat{\pi} \in \mathcal{J}$  or a trivial lower bound like  $t \geq -10^{99}z$ . The purpose of this construction is to guarantee that  $(\hat{\omega}_x, \hat{\omega}_t, \hat{\omega}_0) \in \mathcal{L}^\#$  whenever  $\hat{\omega}_0 = 0$  at Line 3 of Routine 1. Specifically, consider the case where  $\hat{\omega}_0 = 0$  for some  $\omega \in \{\kappa, \nu\}$ . Then, it follows immediately from  $\mathcal{X}_{LP}^\#$  in  $\mathbf{R}$  that  $\hat{\omega}_x = 0$ . Furthermore, the structure of the relaxation of  $\mathcal{L}^\#$  ensures that  $\hat{\omega}_t \geq 0$ . Hence, we conclude that  $\hat{\omega} \in \mathcal{L}^\#$ , validating Line 11. When  $\hat{\omega}_0 > 0$ , based on Proposition 2, the routine refines  $\mathbf{R}$  by iteratively adding separating hyperplanes found via a TYPICALORACLE, which returns an indicator variable  $\mathbb{I}$  and a vector  $\boldsymbol{\alpha} = (\alpha_x, \alpha_t, \alpha_0)$  in Line 7. If  $\mathbb{I} = 1$ , indicating that  $(x', t')$  belongs to  $\mathcal{L}$ , then  $\boldsymbol{\alpha} = 0$ , representing a trivially valid inequality. Otherwise,  $\boldsymbol{\alpha}$  defines an inequality  $\alpha_x^\top x + \alpha_t t \geq \alpha_0$  that separates  $(x', t')$  from  $\mathcal{L}$ .

The convergence behavior of Routine 1 depends on the choice of TYPICALORACLE in Line 7. However, as long as the chosen TYPICALORACLE guarantees finite convergence of BENDERSSSEQ for solving (1.1), it likewise ensures the finite convergence of Routine 1. In addition, when TYPICALORACLE( $x', t'$ ) provides  $f(x')$  as a byproduct—such as in the case of the classical Benders cut generation oracle, the termination can be based on optimality gap (Remark 4). More interestingly, even if Routine 1 is terminated before full convergence, the dual solution will still yield a valid disjunctive Benders cut that supports a relaxation of  $\text{conv}(\mathcal{P}^{(\phi, \phi_0)})$  (Proposition 3). Moreover, Routine 1 generates a series of effective Benders cuts as a byproduct by separating automatically perturbed points (Remark 5). Finally, Routine 1 can easily incorporate previously identified disjunctive cuts to generate them in an accumulated manner (Remark 6).

**Remark 4** (Optimality gap-based termination of Routine 1). *Since  $\mathbf{R}$  is a relaxation of (DCGLP), its optimal objective value at each iteration provides a lower bound on the optimal objective value of (DCGLP). Additionally, if TYPICALORACLE( $x', t'$ ) provides  $f(x')$  as a byproduct—such as in the case of a classical Benders cut generation oracle—an upper bound on the optimal objective can be computed at each iteration, allowing the routine to terminate based on the optimality gap. Specifically, after Line 11, if  $\mathbb{I}_{\mathcal{L}^\#}(\omega) = \text{true}$ , then we define  $\omega'_t := \hat{\omega}_t$ . Otherwise, i.e., when  $\hat{\omega}_0 > 0$  and  $\mathbb{I}_{\mathcal{L}^\#}(\omega) = \text{false}$ , if  $f(\hat{\omega}_x/\hat{\omega}_0) < \infty$ , we have  $\max_{\tilde{\pi} \in \mathcal{R}} \tilde{\pi}^\top (b - A(\hat{\omega}_x/\hat{\omega}_0)) \leq 0$ , which implies  $\max_{\tilde{\pi} \in \mathcal{R}} \tilde{\pi}^\top (b\hat{\omega}_0 - A\hat{\omega}_x) \leq 0$ . Furthermore, since  $\hat{\omega}_0 f(\hat{\omega}_x/\hat{\omega}_0) = \max_{\tilde{\pi} \in \mathcal{J}} \tilde{\pi}^\top (b\hat{\omega}_0 - A\hat{\omega}_x)$ , we can modify  $\hat{\omega}_t$  as  $\omega'_t := \hat{\omega}_0 f(\hat{\omega}_x/\hat{\omega}_0)$ , so that  $\hat{\omega} \in \mathcal{L}^\#$ . If  $f(\hat{\omega}_x/\hat{\omega}_0) = \infty$ , we proceed similarly, modifying  $\hat{\omega}_t$  as  $\omega'_t := \hat{\omega}_0 f(\hat{\omega}_x/\hat{\omega}_0) = \infty$ . As a result, the upper bound can be updated by evaluating the objective function at the modified  $(\hat{\kappa}, \hat{\nu})$ , which is now feasible to (DCGLP):  $UB \leftarrow \min\{UB, \|(\hat{s}_x, \kappa'_t + \nu'_t - \hat{t})\|_p\}$ .*

Let  $\rho \in \mathbb{Z}_{>0}$  be the iteration counter of Routine 1, and let  $\mathcal{L}^{(\rho)} \subseteq \mathcal{L}$  denote the refined relaxation

---

**Routine 1** THE ORACLE: disjunctive Benders cut separation oracle

---

**Require:** tolerance  $\epsilon > 0$ ; split  $(\phi, \phi_0)$ ; point  $(\hat{x}, \hat{t})$  to separate

- 1:  $R \leftarrow$  a relaxation of (DCGLP) with  $\mathcal{L}$  replaced by a relaxation of it, including at least one optimality cut or a trivial lower bound on  $t$ ;  $\mathbb{I}_{\mathcal{L}^\#}(\kappa) \leftarrow \text{false}$ ;  $\mathbb{I}_{\mathcal{L}^\#}(\nu) \leftarrow \text{false}$
- 2: **while**  $\mathbb{I}_{\mathcal{L}^\#}(\kappa) \wedge \mathbb{I}_{\mathcal{L}^\#}(\nu)$  **do**
- 3:     Solve  $R$ ;  $(\hat{\kappa}, \hat{\nu}, \hat{s}, \hat{t}) \leftarrow$  its optimal solution
- 4:     **for**  $\omega$  in  $\{\kappa, \nu\}$  **do** in parallel
- 5:         **if**  $\hat{\omega}_0 > \epsilon$  **then**
- 6:              $x' \leftarrow \hat{\omega}_x / \hat{\omega}_0$ ;  $t' \leftarrow \hat{\omega}_t / \hat{\omega}_0$
- 7:              $(\mathbb{I}_{\mathcal{L}^\#}(\omega), (\alpha_x, \alpha_t, \alpha_0)) \leftarrow \text{TYPICALORACLE}(x', t')$
- 8:             **if**  $\mathbb{I}_{\mathcal{L}^\#}(\omega)$  **then**
- 9:                 Add  $\alpha_0 \kappa_0 - \alpha_x^\top \kappa_x - \alpha_t \kappa_t \leq 0$  and  $\alpha_0 \nu_0 - \alpha_x^\top \nu_x - \alpha_t \nu_t \leq 0$  to  $R$
- 10:         **else**
- 11:              $\mathbb{I}_{\mathcal{L}^\#}(\omega) \leftarrow \text{true}$
- 12:      $\hat{\gamma}_0, \hat{\gamma}_x, \hat{\gamma}_t \leftarrow$  dual values of (DCGLP.i), (DCGLP.j) and (DCGLP.k)
- 13: **return**  $(\hat{t}, (\hat{\gamma}_x, \hat{\gamma}_t, \hat{\gamma}_0))$

---

of  $\mathcal{L}$  after  $\rho$  iterations, that is

$$\mathcal{L}^{(\rho)} = \mathcal{L}^{(0)} \cap \left\{ (x, t) \in \mathbb{R}^{n_x+1} : (\alpha_x^{(\rho)})^\top x + \alpha_t^{(\rho)} t \geq \alpha_0^{(\rho)}, \quad \rho \in \{0, 1, \dots, 2\rho - 1\} \right\},$$

where  $\mathcal{L}^{(0)}$  is the initial relaxation. For each  $\rho' \in [\rho]$ , the vectors  $\alpha^{(2\rho'-2)}$  and  $\alpha^{(2\rho'-1)}$  correspond to the separating hyperplanes for  $\mathcal{L}$  identified in Line 7 during iteration  $\rho'$ ; if Line 7 is not executed for some  $\omega \in \{\kappa, \nu\}$ , the respective  $\alpha$  is simply a zero vector. Let  $R^{(\rho)}$  denote  $R$  after  $\rho$  iterations, defined as (DCGLP) with  $\mathcal{L}^\#$  replaced by  $(\mathcal{L}^{(\rho)})^\#$ , a raised version of  $\mathcal{L}^{(\rho)}$ . Let  $(\kappa^{(\rho)}, \nu^{(\rho)}, s^{(\rho)}, \tau^{(\rho)})$  be the optimal solution of  $R^{(\rho)}$ , and let  $\gamma^{(\rho)}$  denote the optimal dual solution of  $R^{(\rho)}$  associated with (DCGLP.i)-(DCGLP.k).

Since  $R^{(\rho)}$  is a relaxation of (DCGLP), its dual serves as a restriction of (CGLP). Consequently, the intermediate value  $\gamma^{(\rho)}$  still provides a valid inequality for (1.1). This is formally stated in the following proposition:

**Proposition 3.**  $R^{(\rho)}$  corresponds to a projection problem:

$$\tau^{(\rho)} = \min \| (x, t) - (\hat{x}, \hat{t}) \|_p : (x, t) \in \text{conv}((\mathcal{P}^{(\rho)})^{(\phi, \phi_0)}),$$

where  $\mathcal{P}$  in (DCGLP) is replaced by  $\mathcal{P}^{(\rho)} = (\mathcal{X}_{LP} \times \mathbb{R}) \cap \mathcal{L}^{(\rho)}$ . Therefore, at each intermediate iteration  $\rho \in \mathbb{Z}_{\geq 0}$  with  $\tau^{(\rho)} > 0$ , the point  $(\kappa_x^{(\rho)} + \nu_x^{(\rho)}, \kappa_t^{(\rho)} + \nu_t^{(\rho)})$  is the projection of  $(\hat{x}, \hat{t})$  onto  $\text{conv}((\mathcal{P}^{(\rho)})^{(\phi, \phi_0)})$ . The inequality  $\gamma_0^{(\rho)} - (\gamma_x^{(\rho)})^\top x - \gamma_t^{(\rho)} t \leq 0$  defines a supporting hyperplane to  $\text{conv}((\mathcal{P}^{(\rho)})^{(\phi, \phi_0)}) \supseteq \text{conv}(\mathcal{P}^{(\phi, \phi_0)})$  that separates  $(\hat{x}, \hat{t})$ .

Proposition 3 suggests that solving (DCGLP) inexactly—by terminating Routine 1 early and adding the cut derived from the intermediate solution—remains valid. The following example illustrates Proposition 3 while showing how disjunctive Benders cuts are found via Routine 1:

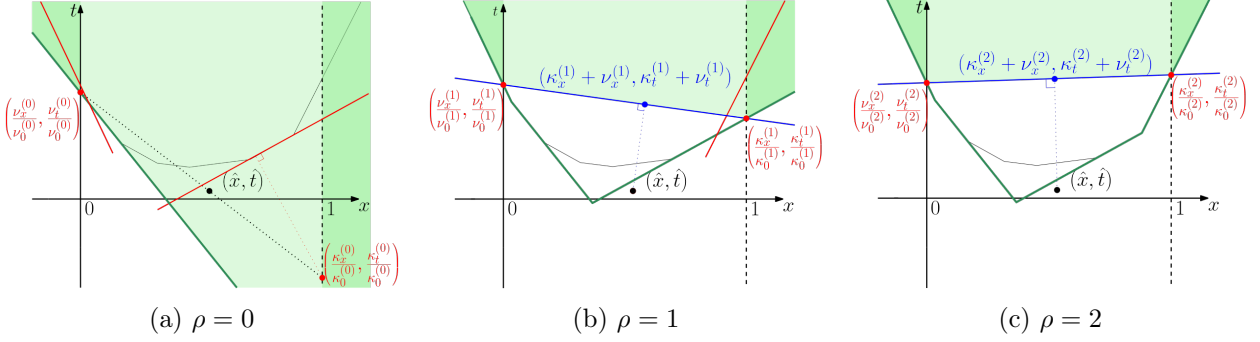


Figure 3: Visualization of Routine 1 over iterations

**Example 1.** Consider an example illustrated in Figure 3a, where  $\mathcal{X} = \mathbb{Z}$  and  $\text{dom } f = \mathbb{R}$ . The solid thin black line represents the graph of the value function  $f$ , and  $(\hat{x}, \hat{t})$  is the point to be separated. The set  $\mathcal{L}$  corresponds to the epigraph of  $f$ , and its initial relaxation  $\mathcal{L}^{(0)}$  contains a single optimality cut, shown as the green line in Figure 3a. Suppose we use the split  $(\phi, \phi_0) = (1, 0)$ , which induces the disjunction  $x \leq 0 \vee x \geq 1$ . Figure 3 illustrates the progress of Routine 1 when it uses the  $\|\cdot\|_2$ -norm for (CGLP) and employs a TYPICALORACLE that generates the deepest optimality cut based on the  $\|\cdot\|_2$ -norm in Line 7 (see [22] for details on the TYPICALORACLE). Let  $\rho$  denote the iteration counter of Routine 1, and define the following sets:  $\mathcal{P}^{(\rho)} = (\mathcal{X}_{LP} \times \mathbb{R}) \cap \mathcal{L}^{(\rho)}$ ,  $\mathcal{P}_1^{(\rho)} = \mathcal{P}^{(\rho)} \cap \{(x, t) : x \geq 1\}$ ,  $\mathcal{P}_2^{(\rho)} = \mathcal{P}^{(\rho)} \cap \{(x, t) : x \leq 0\}$ , and  $(\mathcal{P}^{(\rho)})^{(\phi, \phi_0)} = \mathcal{P}_1^{(\rho)} \cup \mathcal{P}_2^{(\rho)}$ . In the figure, the dark green shaded region represents  $(\mathcal{P}^{(\rho)})^{(\phi, \phi_0)}$ , while the combined area of the dark and light green shading corresponds to its convex hull.

Initially,  $(\hat{x}, \hat{t}) \in \mathcal{L}^{(0)}$  and is a convex combination of  $(\kappa_x^{(0)}/\kappa_0^{(0)}, \kappa_t^{(0)}/\kappa_0^{(0)}) \in \mathcal{P}_1^{(0)}$  and  $(\nu_x^{(0)}/\nu_0^{(0)}, \nu_t^{(0)}/\nu_0^{(0)}) \in \mathcal{P}_2^{(0)}$  as depicted in Figure 3a. Line 7 then generates the two red lines illustrated in Figure 3a to separate  $(\nu_x^{(0)}/\nu_0^{(0)}, \nu_t^{(0)}/\nu_0^{(0)})$  and  $(\kappa_x^{(0)}/\kappa_0^{(0)}, \kappa_t^{(0)}/\kappa_0^{(0)})$  from  $\mathcal{L}$ . The two red lines refine  $\mathcal{L}^{(0)}$  into  $\mathcal{L}^{(1)}$ , as shown in Figure 3b. At this point,  $(\hat{x}, \hat{t}) \notin \text{conv}((\mathcal{P}^{(1)})^{(\phi, \phi_0)})$ , and the projection of  $(\hat{x}, \hat{t})$  onto  $\text{conv}((\mathcal{P}^{(1)})^{(\phi, \phi_0)})$  is  $(\kappa_x^{(1)} + \nu_x^{(1)}, \kappa_t^{(1)} + \nu_t^{(1)})$ , a convex combination of  $(\kappa_x^{(1)}/\kappa_0^{(1)}, \kappa_t^{(1)}/\kappa_0^{(1)}) \in \mathcal{P}_1^{(1)}$  and  $(\nu_x^{(1)}/\nu_0^{(1)}, \nu_t^{(1)}/\nu_0^{(1)}) \in \mathcal{P}_2^{(1)}$ . The blue line in Figure 3b represents the disjunctive cut generated by the intermediate dual solution  $\gamma^{(1)}$ . *This intermediate cut still eliminates a considerable portion of the set  $\mathcal{L}$ , something that typical oracles cannot achieve.* After one additional iteration, the algorithm identifies the deepest disjunctive Benders cut for  $\mathcal{P}^{(\phi, \phi_0)}$  as shown in Figure 3c.

**Remark 5** (Benders cuts obtained via automatic perturbation). *While identifying a supporting hyperplane to  $\text{conv}(\mathcal{P}^{(\phi, \phi_0)})$  that separates  $(\hat{x}, \hat{t})$ , Routine 1 also produces Benders cuts for separating  $(x', t')$  from  $\mathcal{L}$  (see Line 7). These byproduct cuts can be integrated into the master problem alongside the disjunctive Benders cut. They can be interpreted as Benders cuts derived by perturbing the separation point  $(\hat{x}, \hat{t})$ , similar to the in-out method [7, 16]. However, unlike the in-out method, which requires a carefully chosen core point, Routine 1 performs this perturbation automatically.*

**Remark 6** (Continual refinement of  $\mathcal{P}$  in (DCGLP)). *Let  $\mathcal{P}'$  denote the set  $\mathcal{P}$  (the continuous relaxation of the feasible region of (1.1)) augmented with a set of  $k$  disjunctive Benders cuts*

---

**Routine 2** THE ORACLE for separable subproblems

---

**Require:** tolerance  $\epsilon > 0$ ; split  $(\phi, \phi_0)$ ; point  $(\hat{x}, \hat{t})$  to separate

- 1:  $R \leftarrow$  a relaxation of (2.6) with  $\mathcal{L}_j$  replaced by a relaxation of it, including at least one optimality cut or a trivial lower bound on  $t$  for all  $j \in [N]$ ;  $\mathbb{I}_{\mathcal{L}_j^\#}(\kappa) \leftarrow \text{false}$ ;  $\mathbb{I}_{\mathcal{L}_j^\#}(\nu) \leftarrow \text{false}$  for all  $j \in [N]$
- 2: **while**  $\neg \bigwedge_{j \in [N]} (\mathbb{I}_{\mathcal{L}_j^\#}(\kappa) \wedge \mathbb{I}_{\mathcal{L}_j^\#}(\nu))$  **do**
- 3:     Solve  $R$ ;  $(\hat{\kappa}, \hat{\nu}, \hat{s}, \hat{\tau}) \leftarrow$  its optimal solution
- 4:     **for**  $\omega$  in  $\{\kappa, \nu\}$  **do** in parallel
- 5:         **if**  $\hat{\omega}_0 > \epsilon$  **then**
- 6:             **for**  $j \in [N]$  **do** in parallel
- 7:                  $x' \leftarrow \hat{\omega}_x / \hat{\omega}_0$ ;  $t'_j \leftarrow \hat{\omega}_{t,j} / \hat{\omega}_0$
- 8:                  $(\mathbb{I}_{\mathcal{L}_j^\#}(\omega), (\alpha_x, \alpha_t, \alpha_0)) \leftarrow \text{TYPICALORACLE}_{\mathcal{L}_j}(x', t'_j)$
- 9:                 **if**  $\neg \mathbb{I}_{\mathcal{L}_j^\#}(\omega)$  **then**
- 10:                     Add  $\alpha_0 \kappa_0 - \alpha_x^\top \kappa_x - \alpha_t^\top \kappa_t \leq 0$  and  $\alpha_0 \nu_0 - \alpha_x^\top \nu_x - \alpha_t^\top \nu_t \leq 0$  to  $R$
- 11:                 **else**
- 12:                      $\mathbb{I}_{\mathcal{L}_j^\#}(\omega) \leftarrow \text{true}$  for all  $j \in [N]$
- 13:      $\hat{\gamma}_0, \hat{\gamma}_x, \hat{\gamma}_t \leftarrow$  dual values of (2.6i), (2.6j) and (2.6k)
- 14: **return**  $(\hat{\tau}, (\hat{\gamma}_x, \hat{\gamma}_t, \hat{\gamma}_0))$

---

$\gamma_0^{(k')} - (\gamma_x^{(k')})^\top x - \gamma_t^{(k')} t \geq 0, k' = 1, \dots, k$ . Then, Routine 1 can generate a disjunctive cut for  $\text{conv}(\mathcal{P}'^{(\phi, \phi_0)}) \subseteq \text{conv}(\mathcal{P}^{(\phi, \phi_0)})$  by incorporating the raised version of the disjunctive cuts, i.e.,  $\gamma_0^{(k')} \kappa_0 - (\gamma_x^{(k')})^\top \kappa_x - \gamma_t^{(k')} \kappa_t \geq 0$  and  $\gamma_0^{(k')} \nu_0 - (\gamma_x^{(k')})^\top \nu_x - \gamma_t^{(k')} \nu_t \geq 0$ , into the relaxation  $R$ , for  $k' \in [k]$ .

### 2.3.1 Decomposable $\text{sub}(\hat{x})$

THE ORACLE can leverage distributed computing resources more effectively when  $\text{sub}(\hat{x})$  decomposes into  $N$  smaller problems, i.e.,  $f(\hat{x}) = \sum_{j \in [N]} f_j(\hat{x})$ , where  $f_j(\hat{x}) := \min_{y_j} \{d_j^\top y_j : B_j y_j \geq b_j - A_j \hat{x}\}$ . Let  $\mathcal{L}_j = \{(x, t_j) \in \mathbb{R}^{n_x+1} : t_j \geq f_j(x), x \in \text{dom } f_j\}$ . It is easy to see that  $(x, t) \in \mathcal{L}$  if and only if there exist  $t_1, \dots, t_N$  such that  $t = \sum_{j \in [N]} t_j, (x, t_j) \in \mathcal{L}_j, \forall j \in [N]$ . Thus, the Benders reformulation (1.1) can be equivalently rewritten by replacing  $t$  with  $\sum_{j \in [N]} t_j$ :

$$\min_{x \in \mathcal{X}, t \in \mathbb{R}} \{c^\top x + \sum_{j \in [N]} t_j : (x, t_j) \in \mathcal{L}_j, \forall j \in [N]\} \quad (2.5)$$

Similarly, for a candidate solution  $(\hat{x}, \hat{t}) \in \mathbb{R}^{n_x} \times \mathbb{R}^N$  obtained from a relaxation of (2.5), the corresponding (DCGLP) can be equivalently expressed as:

$$\min \tau \quad (2.6a)$$

$$\text{s.t. } (\kappa_x, \kappa_{t,j}, \kappa_0) \in \mathcal{L}_j^\#, \forall j \in [N], \quad (2.6b)$$

$$(\kappa_x, \kappa_0) \in \mathcal{X}_{LP}^\#, \quad (2.6c)$$

$$\phi^\top \kappa_x \geq (\phi_0 + 1) \kappa_0, \quad (2.6d)$$

$$(\nu_x, \nu_{t,j}, \nu_0) \in \mathcal{L}_j^\#, \quad \forall j \in [N], \quad (2.6e)$$

$$(\nu_x, \nu_0) \in \mathcal{X}_{LP}^\#, \quad (2.6f)$$

$$-\phi^\top \kappa_x \geq -\phi_0^\top \kappa_0, \quad (2.6g)$$

$$\kappa_0, \nu_0 \geq 0, \quad (2.6h)$$

$$(\gamma_0) \quad \kappa_0 + \nu_0 = 1, \quad (2.6i)$$

$$(\gamma_x) \quad s_x = \kappa_x + \nu_x - \hat{x}, \quad (2.6j)$$

$$(\gamma_{t,j}) \quad s_{t,j} = \kappa_{t,j} + \nu_{t,j} - \hat{t}_j, \quad \forall j \in [N], \quad (2.6k)$$

$$\tau \geq \left\| \begin{pmatrix} s_x \\ (s_{t,j})_{j \in [N]} \end{pmatrix} \right\|_p. \quad (2.6l)$$

This naturally extends Routine 1 to Routine 2, which enables additional parallel computation in Lines 6-10. In Line 8,  $\text{TYPICALORACLE}_{\mathcal{L}_j}$  is any typical Benders oracle that generates a separating hyperplane for  $\mathcal{L}_j$ . All properties of Routine 1 remain valid for this oracle, including optimality-based termination, provided that  $\text{TYPICALORACLE}_{\mathcal{L}_j}$  also returns  $f_j(x')$  for all  $j \in [N]$  (Remark 4). Additionally, intermediate solutions still yield valid disjunctive cuts for (2.5) (Proposition 3). Benders cuts obtained as a byproduct of Routine 2 for each  $j \in [N]$  can be used to enrich the master problem (Remark 5). Additionally, (2.6) can be continually refined by incorporating raised versions of the disjunctive cuts found so far (Remark 6).

## 2.4 Disjunctive Benders decomposition

For the remainder of this paper, we say that a point  $(\hat{x}, \hat{t})$  is integral if  $\hat{x}_j \in \mathbb{Z}$  for all  $j \in \mathcal{I}$ ; otherwise, we call it fractional. THE ORACLE can be used to separate both integral and fractional candidate solutions, provided that the split  $(\phi, \phi_0)$  is chosen such that  $(\hat{x}, \hat{t}) \notin \text{conv}(\mathcal{P}^{(\phi, \phi_0)})$ . However, selecting such a split  $(\phi, \phi_0)$  for an integral  $(\hat{x}, \hat{t})$  is not always straightforward. As a result, we primarily focus on adding disjunctive Benders cuts to separate fractional  $(\hat{x}, \hat{t})$ .

We refer to BD equipped with THE ORACLE, i.e., Routine 1 or 2, as *disjunctive Benders decomposition*. There are multiple ways to integrate disjunctive Benders cuts into BENDERSSEQ and BENDERSBNB. For instance, in BENDERSSEQ, one can solve the continuous relaxation of the master problem, and if the resulting candidate solution  $(\hat{x}, \hat{t})$  is fractional, use THE ORACLE to generate a disjunctive Benders cut for some split  $(\phi, \phi_0)$  that excludes  $\hat{x}$ . If the separation is unsuccessful (which may occur for problems with non-binary integer variables, regardless of the choice of the split; see the example in [14]) or if the candidate solution is integral, a TYPICALORACLE can be called for proper termination. Similarly, in BENDERSBNB, disjunctive Benders cuts can be added at fractional nodes, i.e., nodes where the associated LP subproblems yield fractional candidate solutions, of the branch-and-bound tree. Since THE ORACLE incorporates integrality information that was previously kept within the master problem, the generated cuts can be significantly stronger (see Figure 3).

More interestingly, for certain special cases of (MILP), such as mixed-binary linear programs,

---

**Algorithm 3** A specialized disjunctive BENDERSSEQ for mixed-binary linear programs

---

```

1:  $k \leftarrow 0$ ;  $\mathbf{M} \leftarrow$  a continuous relaxation of (1.1) with a subset of (1.1c) and (1.1b).
2: while true do
3:   Find an optimal basic solution  $(\hat{x}, \hat{t})$  of  $\mathbf{M}$ 
4:    $(\mathbb{I}_{\mathcal{L}}(\hat{x}, \hat{t}), (\alpha_x, \alpha_t, \alpha_0)) \leftarrow \text{TYPICALORACLE}(\hat{x}, \hat{t})$ 
5:   if  $\mathbb{I}_{\mathcal{L}}(\hat{x}, \hat{t})$  then Add  $\alpha_x^\top x + \alpha_t t \leftarrow \alpha_0$  to  $\mathbf{M}$ .
6:   else
7:      $(x^{(k)}, t^{(k)}) \leftarrow (\hat{x}, \hat{t})$ 
8:     if  $x_j^{(k)} \in \{0, 1\}, \forall j \in \mathcal{I}$  then break
9:     (Split selection)  $(\phi, \phi_0) \leftarrow (e_i, 0)$ , where  $i$  is the largest index in  $\mathcal{I} = \{1, \dots, \ell\}$  such that
     $0 < \hat{x}_i^{(k)} < 1$ , i.e.,  $\hat{x}_j^{(k)} \in \{0, 1\}$  for all  $j = i + 1, \dots, \ell$ .
10:    (Initialization of (DCGLP)) Construct (DCGLP) for the split  $(\phi, \phi_0)$  with an initial relaxation
    of  $\mathcal{L}$ ; include the raised version of all previously found disjunctive cuts for splits  $(e_j, 0)$  where
     $j = 1, \dots, i - 1$  (see Remark 6).
11:     $(\hat{\tau}, (\hat{\gamma}_x, \hat{\gamma}_t, \hat{\gamma}_0)) \leftarrow \text{THE ORACLE}((\phi, \phi_0), (x^{(k)}, t^{(k)}))$ 
12:    Add  $\hat{\gamma}_x^\top x + \hat{\gamma}_t t \geq \hat{\gamma}_0$  to  $\mathbf{M}$ 
13:     $k \leftarrow k + 1$ 
return  $x^{(k)}$ 

```

---

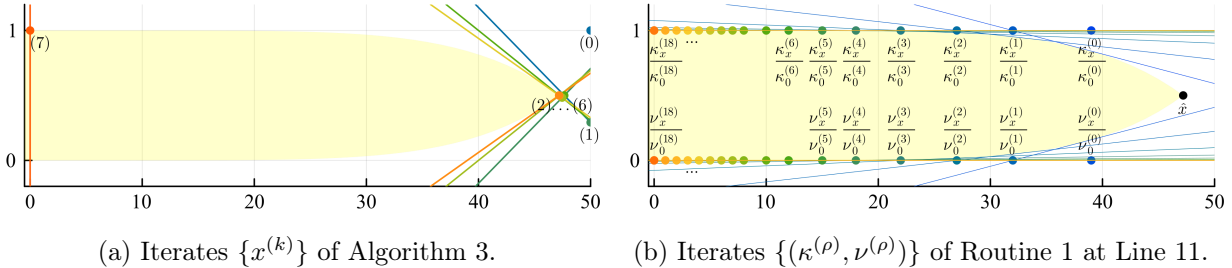


Figure 4: Illustration of Algorithm 3 on the motivating example with colors associate the iterates and cuts.

a specialized strategy for constructing splits and leveraging previously found disjunctive cuts (see Algorithm 3) can entirely eliminate the need to solve the master problem as a MILP in BENDERSSEQ. In other words, in BENDERSBNB, it can prevent the branch-and-bound tree from expanding beyond the root node, enabling termination at the root.

**Theorem 1.** *Suppose (MILP) is a mixed-binary linear program, i.e.,  $[l_j, u_j] = [0, 1]$  for all  $j \in \mathcal{I}$  and  $p \in \{1, \infty\}$ . Then, Algorithm 3 yields an optimal solution to (1.1) in a finite number of iterations.*

**Remark 7.** *Theorem 1 is a significant result, as it implies that disjunctive Benders decomposition can eliminate the need to solve the master problem as a MILP in BENDERSSEQ, thereby removing the primary computational bottleneck for large-scale problems. Moreover, it suggests that in BENDERSBNB, the algorithm can terminate at the root node without further branching, highlighting its potential to significantly reduce the size of the branch-and-bound tree.*

**Example 2.** Consider applying Algorithm 3 to the motivating example in Section 1.2, despite the

lack of a finite convergence guarantee due to  $x_2$  being a general integer variable. As shown in Figure 4a, the algorithm first adds seven Benders cuts until it identifies the optimal solution  $x^{(6)} = (47.2, 0.5)$  to the LP relaxation of (1.1). At this point, it executes Line 8, constructs the split  $(e_2, 0)$  in Line 9, and initiate the approximation of  $\mathcal{L}$  with the seven Benders cuts in (DCGLP). Routine 1 then generates the disjunctive Benders cut  $x_1 \geq 0$ , immediately leading to the identification of the optimal solution after incorporating just one disjunctive cut. Interestingly, as shown in Figure 4b, Benders cuts identified in Line 7 of Routine 1—in the process of generating the disjunctive cut—closely resemble those produced by BENDERSSEQ (see Figure 2b). However, this result is particularly noteworthy given the fundamental difference in the types of relaxed problems each approach solves: Algorithm 3 exclusively solves continuous problems, whereas classical BENDERSSEQ requires solving a mixed-integer master problem at each iteration. As a result, the potential computational savings can be substantial.

### 3 Further improvements for mixed-binary linear programs

In a mixed-binary linear program, where  $[l_j, u_j] = [0, 1]$  for  $j \in \mathcal{I}$ , a disjunctive cut derived from a simple split  $(\phi, \phi_0) = (e_i, 0)$  for some  $i \in \mathcal{I}$  is known as a lift-and-project cut [6]. This type of cut can be strengthened *a posteriori* by exploiting the integrality of other binary variables. Additionally, a lift-and-project cut derived from a subproblem associated with a specific branch-and-bound node can be lifted to ensure its validity across the entire branch-and-bound tree [4]. We extend this idea to the disjunctive Benders decomposition in a way that enables straightforward implementation. This extension further motivates the development of an approximate version of THE ORACLE for generating lift-and-project cuts, which provides computational benefits. Throughout this section, we consider (DCGLP) constructed based on a simple split  $(\phi, \phi_0) = (e_i, 0)$  for some  $i \in \mathcal{I}$ , and assume that the generated disjunctive Benders cut  $\hat{\gamma}_0 - \hat{\gamma}_x^\top x - \hat{\gamma}_t t \leq 0$  cuts off the current iterate  $(\hat{x}, \hat{t})$ .

#### 3.1 Cut strengthening

Let  $\hat{\gamma} = (\hat{\gamma}_0, \hat{\gamma}_x, \hat{\gamma}_t)$ ,  $\hat{\sigma}^1$ , and  $\hat{\sigma}^2$  be the dual solutions associated with (DCGLP.i)-(DCGLP.k), (DCGLP.d), and (DCGLP.g), respectively. If  $\hat{\sigma}^1 + \hat{\sigma}^2 > 0$ , we can strengthen the cut  $\hat{\gamma}_0 - \hat{\gamma}_x^\top x - \hat{\gamma}_t t \leq 0$  as

$$\gamma'_0 - (\gamma'_x)^\top x - \gamma'_t t \leq 0 \quad (3.1)$$

with

$$\begin{cases} \gamma'_0 = \hat{\gamma}_0, \\ \gamma'_{x,j} = \min \left\{ \hat{a}_j^1 - \hat{\sigma}^1 \left\lfloor \frac{\hat{a}_j^1 - \hat{a}_j^2}{\hat{\sigma}^1 + \hat{\sigma}^2} \right\rfloor, \hat{a}_j^2 + \hat{\sigma}^2 \left\lceil \frac{\hat{a}_j^1 - \hat{a}_j^2}{\hat{\sigma}^1 + \hat{\sigma}^2} \right\rceil \right\}, \quad \forall j \in \mathcal{I}, \\ \gamma'_{x,j} = \hat{\gamma}_{x,j}, \quad \forall j \in [n_x] \setminus \mathcal{I}, \\ \gamma'_t = \hat{\gamma}_t, \end{cases}$$

where  $\hat{a}_j^1 = (\hat{\gamma}_x)_j - \hat{\delta}_j^1$  and  $\hat{a}_j^2 = (\hat{\gamma}_x)_j - \hat{\delta}_j^2$  for  $j \in \mathcal{I}$  with  $\hat{\delta}_j^1$  and  $\hat{\delta}_j^2$  being the dual solutions associated with the nonnegativity constraints  $(\kappa_x)_j \geq 0$  and  $(\nu_x)_j \geq 0$  respectively.

**Proposition 4.** *If  $\hat{\sigma}^1 + \hat{\sigma}^2 > 0$ , (3.1) is valid inequality for (1.1) and tighter than  $\hat{\gamma}_0 - \hat{\gamma}_x^\top x - \hat{\gamma}_t t \leq 0$ .*

**Remark 8.** *The proof implies that this strengthening procedure remains valid for suboptimal solutions of (DCGLP), i.e., an intermediate point in Routine 1 or 2 with  $\hat{\tau}^{(\rho)} > 0$ . One can simply retrieve the dual solutions for  $R^{(\rho)}$  and apply the same strengthening procedure.*

### 3.2 Cut lifting

THE ORACLE, i.e., Routine 1 or 2, can be called at any fractional node of a branch-and-bound tree when solving (1.1) in the BENDERSBNB framework. Each node  $n$  of a branch-and-bound tree is associated with a pair of disjoint index sets  $(\mathcal{I}_{n,0}, \mathcal{I}_{n,1})$ , where  $\mathcal{I}_{n,l}$  denotes the set of indices of binary variables which values are fixed at  $l$  at the node. A cut that is generated at  $n$  can be extended to be valid for (1.1) by adjusting coefficients for the variables  $x_j$  where  $j \in \mathcal{I}_n := \mathcal{I}_{n,0} \cup \mathcal{I}_{n,1}$  and the right-hand side. This process is referred to as *lifting* the cut. In this section, we propose a simple postprocessing step for lifting the disjunctive Benders cut.

We denote the feasible region of the LP subproblem at a fractional node  $n$  as  $\mathcal{P}_n := \mathcal{P} \cap \{(x, t) \in \mathbb{R}^{nx+1} : -x_j \geq 0, \forall j \in \mathcal{I}_{n,0}, x_j \geq 1, \forall j \in \mathcal{I}_{n,1}\}$ . Let  $(\hat{x}, \hat{t})$  be the fractional local solution. To simplify notation, let  $\mathcal{P}_{i,n} := \mathcal{P}_n^{(e_i, 0)}$  and  $\mathcal{P}_i := \mathcal{P}^{(e_i, 0)}$ . A disjunctive Benders cut for separating  $(\hat{x}, \hat{t})$  from  $\mathcal{P}_{i,n}$ , i.e., the local problem, can be derived by solving (DCGLP) with the addition of the following constraints:

$$(\zeta^1) \quad 0 \geq (\kappa_x)_j, \quad \forall j \in \mathcal{I}_{n,0} \quad (3.2a)$$

$$(\xi^1) \quad 0 \geq \kappa_0 - (\kappa_x)_j, \quad \forall j \in \mathcal{I}_{n,1} \quad (3.2b)$$

$$(\zeta^2) \quad 0 \geq (\nu_x)_j, \quad \forall j \in \mathcal{I}_{n,0} \quad (3.2c)$$

$$(\xi^2) \quad 0 \geq \nu_0 - (\nu_x)_j, \quad \forall j \in \mathcal{I}_{n,1}. \quad (3.2d)$$

We refer to the resulting augmented problem as  $(DCGLP_n)$ . Suppose  $(\gamma, \chi, \zeta, \xi)$  be a dual solution of  $(DCGLP_n)$ . The corresponding cut  $\gamma_0 - \gamma_x^\top x - \gamma_t t \leq 0$  valid for  $\mathcal{P}_{i,n}$  can be lifted to be valid for  $\mathcal{P}_i$  as follows:

$$\hat{\gamma}_0 - \hat{\gamma}_x^\top x - \hat{\gamma}_t t \leq 0, \quad (3.3)$$

where

$$\begin{aligned} \hat{\gamma}_t &= \gamma_t, \\ \hat{\gamma}_0 &= \gamma_0 - \sum_{j \in \mathcal{I}_{n,1}} \max\{\xi_j^1, \xi_j^2\}, \end{aligned}$$

$$\widehat{\gamma}_x, j = \begin{cases} \gamma_{x,j}, & \forall j \notin \mathcal{I}_n, \\ \gamma_{x,j} + \max\{\zeta_j^1, \zeta_j^2\}, & \forall j \in \mathcal{I}_{n,0}, \\ \gamma_{x,j} - \max\{\xi_j^1, \xi_j^2\}, & \forall j \in \mathcal{I}_{n,1}. \end{cases}$$

**Proposition 5.** *The lifted inequality (3.3) is valid for  $\mathcal{P}_i = \mathcal{P}^{(e_i, 0)}$ , i.e., it is valid for any nodes of the branch-and-bound tree. In addition, it still cuts off the local solution  $(\hat{x}, \hat{t})$ , specifically  $\widehat{\gamma}_0 - \widehat{\gamma}_x^\top \hat{x} - \widehat{\gamma}_t \hat{t} = \gamma_0 - \gamma_x^\top \hat{x} - \gamma_t \hat{t} > 0$ . Specifically, the lifted  $\widehat{\gamma}$  satisfies (2.1) with  $\widehat{\chi}$ , given as*

$$\forall r \in \{1, 2\}, ((\widehat{\lambda}_{\hat{\pi}}^r)_{\hat{\pi} \in \mathcal{J}}, (\widehat{\mu}_{\hat{\pi}}^r)_{\hat{\pi} \in \mathcal{R}}, \widehat{\theta}^r, \widehat{\sigma}^r) = ((\lambda_{\hat{\pi}}^r)_{\hat{\pi} \in \mathcal{J}}, (\mu_{\hat{\pi}}^r)_{\hat{\pi} \in \mathcal{R}}, \theta^r, \sigma^r), \quad (3.4a)$$

$$\widehat{\delta}_j^r = \delta_j^r - \zeta_j^r + \max\{\zeta_j^1, \zeta_j^2\}, \quad \forall j \in \mathcal{I}_{n,0}, \quad (3.4b)$$

$$\widehat{\eta}_j^r = \eta_j^r - \xi_j^r + \max\{\xi_j^1, \xi_j^2\}, \quad \forall j \in \mathcal{I}_{n,1}. \quad (3.4c)$$

**Remark 9.** *The original lifting procedure for generic mixed-binary linear programs [4, 5] assumes that  $\mathcal{I}_{n,1} = \emptyset$  by working directly with the transformed polyhedron  $g(\mathcal{P}_i)$  (see (A.2) for the definition of  $g$ ). However, the lifted cut resulting from this transformation is not easily applicable within the disjunctive Benders framework, as it requires the primal and dual solution pair for the transformed  $(DCGLP_n)$ , which can be cumbersome to implement. In contrast, we show in Lemma A-1 that the affine transformation preserves the Farkas multiplier, and use this property to provide a simple method for directly lifting a disjunctive cut. This method avoids the complex matrix and vector conversions required in  $(DCGLP_n)$  to make  $\mathcal{I}_{n,1} = \emptyset$ , instead relying on a retrieval of the dual solution from  $(DCGLP_n)$  and applying a simple elementary operation, as outlined in (3.3).*

**Remark 10.** *A lifted inequality can be further strengthened by applying the strengthening technique presented in Section 3.1. One can simply apply (3.1) to  $(\widehat{\gamma}, \widehat{\chi})$ , as given in (3.3) and (3.4), to obtain the strengthened lifted cut.*

### 3.3 THE APPROXORACLE: an approximate version of THE ORACLE

Proposition 5 motivates an approximate version of THE ORACLE for generating lift-and-project cuts, which offers computational efficiency while guaranteeing the generation of a hyperplane that separates  $(\hat{x}, \hat{t})$  from  $\text{conv}(\mathcal{P}^{(\phi, \phi_0)})$  if and only if  $(\hat{x}, \hat{t}) \notin \text{conv}(\mathcal{P}^{(\phi, \phi_0)})$ .

**Theorem 2.** *Let  $(\tau, \widehat{\gamma})$  be the output of Routine 4. Consider  $(CGLP)$  constructed for the split  $(e_i, 0)$  and the point  $(\hat{x}, \hat{t})$ , and let  $v_{(CGLP)}$  be its optimal objective value. Then,  $v_{(CGLP)} \leq \tau$ . Additionally, the scaled solution  $\frac{1}{\max\{\|(\widehat{\gamma}_x, \widehat{\gamma}_t)\|_q, 1\}} \widehat{\gamma}$  is feasible to  $(CGLP)$  and evaluates its objective function at  $\tau \frac{1}{\max\{\|(\widehat{\gamma}_x, \widehat{\gamma}_t)\|_q, 1\}}$ , providing  $v_{(CGLP)} \geq \frac{\tau}{\max\{\|(\widehat{\gamma}_x, \widehat{\gamma}_t)\|_q, 1\}}$ . Therefore, the solution  $\widehat{\gamma}$  generated by THE APPROXORACLE, when scaled by  $\frac{1}{\max\{\|(\widehat{\gamma}_x, \widehat{\gamma}_t)\|_q, 1\}}$ , is  $\left(1 - \frac{1}{\max\{\|(\widehat{\gamma}_x, \widehat{\gamma}_t)\|_q, 1\}}\right)$ -optimal to  $(CGLP)$ .*

**Remark 11.** *When a fractional  $\hat{x}$  has many integral components, THE APPROXORACLE can be significantly more computationally efficient than THE ORACLE, as it restricts the feasible region*

---

**Routine 4** THE APPROXORACLE for generating a lift-and-project cut

---

**Require:** tolerance  $\epsilon > 0$ ; split  $(e_i, 0)$ ; point  $(\hat{x}, \hat{t})$  to separate, where  $\hat{x}_i \in (0, 1)$

- 1: Perform Line 1 in Routine 1
- 2:  $\mathcal{I}_r \leftarrow \{j \in \mathcal{I} : \hat{x}_j = r\}$  for  $r \in \{0, 1\}$
- 3: Add to  $\mathbf{R}$  the inequalities (3.2), replacing  $\mathcal{I}_{n,r}$  with  $\mathcal{I}_r$  for  $r \in \{0, 1\}$
- 4: Execute Lines 2–11 of Routine 1
- 5:  $\tau \leftarrow$  optimal objective value of  $\mathbf{R}$ ;  $(\gamma, (\xi, \zeta)) \leftarrow$  optimal dual solutions associated with (DCGLP.i)–(DCGLP.k) and (3.2) respectively in  $\mathbf{R}$
- 6: Compute  $\hat{\gamma}$  using (3.3) applied to  $(\gamma, \xi, \zeta)$
- 7: **return**  $(\tau, (\hat{\gamma}_x, \hat{\gamma}_t, \hat{\gamma}_0))$

---

*substantially. Nevertheless, it guarantees the generation of a separating hyperplane if and only if  $(\hat{x}, \hat{t}) \notin \text{conv}(\mathcal{P}^{(\phi, \phi_0)})$ , ensuring proper termination; note that  $\tau$  can be zero if and only if  $(\hat{x}, \hat{t}) \in \text{conv}(\mathcal{P}^{(\phi, \phi_0)})$  due to Theorem 2. Furthermore, the cut generated by THE APPROXORACLE can be further strengthened following the approach in Remark 10.*

## 4 Discussion

THE ORACLE provides a recipe for leveraging existing typical Benders oracles—those that separate a point from  $\mathcal{L}$ —to discover valid inequalities for  $\text{conv}((\mathcal{X} \times \mathbb{R}) \cap \mathcal{L})$ . It actively identifies previously unknown constraints that are crucial for finding a supporting hyperplane to a set that lies between  $\text{conv}((\mathcal{X} \times \mathbb{R}) \cap \mathcal{L})$  and  $\mathcal{L}$ . This approach contrasts sharply with other methods that rely on pre-generated Benders cuts to construct valid inequalities (e.g., mixed-integer rounding enhancement [11]); while such methods can be handled internally by off-the-shelf solvers to some extent, they can also be combined with the proposed approach for enhanced effectiveness. In this section, we compare the proposed method with existing oracles that fall into the category shown in Figure 1b, which do not rely solely on pre-generated Benders cuts. For simplicity, we assume for the rest of this section that  $\mathcal{I} = [n_x]$  and  $\text{dom } f_j = \mathbb{R}^{n_x}$  for all  $j \in [N]$ , i.e., the subproblems have complete recourse. The discussion that will follow will remain true in general cases without the assumption.

The project-and-cut approach proposed in [10] also aims to generate a disjunctive cut for (1.1). To address the incomplete characterization of  $\mathcal{L}$  in the evolving master problem—a relaxation of (1.1)—during BD, they propose solving a cut-generating LP constructed from the original formulation (MILP). However, this approach can be computationally demanding for large-scale problems, as the CGLP typically doubles the size of the original problem or is at least as large as the original formulation. Possibly due to this computational burden, their experiment focuses on generating disjunctive cuts for the current master problem, only using the current relaxation of  $\mathcal{L}$ .

In the context of THE ORACLE, this corresponds to the initial iteration of Routine 1 or 2 applied to a relaxation of (DCGLP), initialized with the added Benders cuts to the master problem. Consequently, the resulting cut is weaker than the one produced by THE ORACLE, which, *beyond the initial iteration, iteratively discovers unknown Benders cuts to generate a stronger disjunctive cut*.

They also experiment with solving the CGLP for the original formulation on a per-scenario basis, possibly to mitigate the problem size explosion as more scenarios are incorporated. In contrast, Routine 2 can harness parallel computing resources effectively to generate the deepest disjunctive cut with all the scenarios taken into account simultaneously.

The cut-and-project approach in [10] and the Lagrangian cut in [31, 35] are inspired by the following Lagrangian relaxation of (1.1) typically used in dual decomposition:

$$\min c^\top x + \sum_{j \in [N]} t_j \quad (4.1a)$$

$$\text{s.t. } (x, t_j) \in \text{conv}((\mathcal{X} \times \mathbb{R}) \cap \mathcal{L}_j), \forall j \in [N], \quad (4.1b)$$

where  $(\mathcal{X} \times \mathbb{R}) \cap \mathcal{L}_j = \{(x, t_j) : t_j \geq f_j(x), x \in \mathcal{X}\}$ . Both the cut-and-project approach and the Lagrangian cut aim to separate a candidate solution  $(\hat{x}, \hat{t}_j)$  of (4.1) from  $\text{conv}((\mathcal{X} \times \mathbb{R}) \cap \mathcal{L}_j)$  whenever  $(\hat{x}, \hat{t}_j) \notin \text{conv}((\mathcal{X} \times \mathbb{R}) \cap \mathcal{L}_j)$  for each  $j \in [N]$ . They generate cuts based on two different descriptions of  $\text{conv}((\mathcal{X} \times \mathbb{R}) \cap \mathcal{L}_j)$ . Specifically, the cut-and-project approach uses the following description:

$$\begin{aligned} \text{conv}((\mathcal{X} \times \mathbb{R}) \cap \mathcal{L}_j) &= \text{conv}(\{(x, t_j) : t_j \geq f_j(x), x \in \mathcal{X}\}) \\ &= \text{conv}(\{(x, t_j) : \exists y_j \text{ such that } (x, t_j, y_j) \in \mathcal{Q}_j\}), \\ &= \text{conv}(\text{Proj}_{(x, t_j)} \mathcal{Q}_j) \\ &= \text{Proj}_{(x, t_j)}(\text{conv}(\mathcal{Q}_j)), \end{aligned} \quad (4.2)$$

where  $\mathcal{Q}_j := \{(x, t_j, y_j) : t_j \geq d_j^\top y_j, A_j x + B_j y_j \geq b_j, x \in \mathcal{X}\}$ , and the last equality is from [13, Exercise 3.34]. On the other hand, the Lagrangian cut leverages the following alternative description of  $\text{conv}((\mathcal{X} \times \mathbb{R}) \cap \mathcal{L}_j)$ :

$$\text{conv}((\mathcal{X} \times \mathbb{R}) \cap \mathcal{L}_j) = \text{conv}(\{(x, t_j) : t_j \geq f_j(x), x \in \mathcal{X}\}) = \text{conv}(\text{epi } f'_j) = \text{epi}(f'^{**}_j),$$

where  $f'_j$  is a function that equals  $f_j(x)$  for  $x \in \mathcal{X}$  and  $\infty$  otherwise;  $f'^{**}_j$  is the biconjugate of  $f'_j$ , whose epigraph is the closure of the convex hull of the epigraph of  $f'_j$  [8, Proposition 1.6.1]. The last equality follows from the closedness of  $\text{conv}(\text{epi } f'_j)$ , which follows from the lower semicontinuity of  $f'_j$  and the compactness of  $\mathcal{X}$ . Since we have

$$\begin{aligned} f'^{**}_j(x) &= \max_{\pi_j} \pi_j^\top x - f'^*_j(\pi) = \max_{\pi_j} \pi_j^\top x + \min_{z_j} f'_j(z_j) - \pi_j^\top z_j = \max_{\pi_j} \pi_j^\top x + \min_{z_j \in \mathcal{X}} f_j(z_j) - \pi_j^\top z_j \\ &= \max_{\pi_j} \pi_j^\top x + \min_{z_j \in \mathcal{X}, y_j} d_j^\top y_j - \pi_j^\top z_j : A_j z_j + B_j y_j \geq b_j, \end{aligned}$$

it follows that

$$\text{conv}((\mathcal{X} \times \mathbb{R}) \cap \mathcal{L}_j) = \{(x, t_j) : t_j \geq \max_{\pi_j} \pi_j^\top x + \min_{z_j \in \mathcal{X}, y_j} \{d_j^\top y_j - \pi_j^\top z_j : A_j z_j + B_j y_j \geq b_j\}\}. \quad (4.3)$$

Given a point  $(\hat{x}, (\hat{t}_j)_{j \in [N]})$  to separate, the cut-and-project approach, based on (4.2), repeatedly (i) solves  $(\text{sub}(\hat{x}))$  to obtain the optimal  $\hat{y}_j$  with the optimal objective value  $f_j(\hat{x})$ , (ii) generates an inequality that separates the point  $(\hat{x}, \hat{f}_j(\hat{x}), \hat{y}_j)$  from  $\text{conv } \mathcal{Q}_j$ , if such an inequality exists, and (iii) incorporates the inequality into  $(\text{sub}(\hat{x}))$ . Upon termination, the Benders cut is derived from the final modified subproblem. The Lagrangian cut, based on (4.3), is constructed by first determining a (sub)optimal  $\hat{\pi}_j$  for the maximization problem in (4.3) given  $\hat{x}$ . Then, the inner MILP subproblem is solved to obtain an optimal solution  $(\hat{y}_j, \hat{z}_j)$  for the given  $\hat{\pi}_j$  and  $\hat{x}$ . Finally, the cut  $t_j \geq \hat{\pi}_j^\top (x - \hat{z}_j) + d_j^\top \hat{y}_j$  is generated.

It is well known that (4.1) is equivalent to (1.1) only when  $N = 1$ , and it serves as a relaxation whenever  $N > 1$ , as  $\bigcap_{j \in [N]} \text{conv}((\mathcal{X} \times \mathbb{R}) \cap \mathcal{L}_j) \supseteq \text{conv}((\mathcal{X} \times \mathbb{R}) \cap \bigcap_{j \in [N]} \mathcal{L}_j)$ . Due to this, by design, the oracles generating the Lagrangian cuts and the cut-and-project cuts do not eliminate the need to solve the master problem as an MILP unless  $N = 1$ . In contrast, the proposed disjunctive Benders decomposition can completely eliminate the need to solve the master problem as an MILP for any  $N \in \mathbb{Z}_{>0}$  for mixed-binary linear programs (see, e.g., Theorem 1). Additionally, THE ORACLE identifies effective Benders cuts for each scenario as a byproduct of finding the deepest disjunctive cut for (1.1). These cuts can be further incorporated into the master problem.

Furthermore, even in the nonseparable case, that is  $N = 1$ , THE ORACLE can be more effective at managing problem scale. Generating Lagrangian cuts for  $\text{conv}((\mathcal{X} \times \mathbb{R}) \cap \mathcal{L}_j)$  requires solving MILP subproblems, which may not scale well for large problems. Similarly, in the cut-and-project scheme, when  $N = 1$ , the process reduces to generating valid cuts for the original formulation (MILP), which can also face scalability limitations. In contrast, THE ORACLE requires only iterations of typical oracles, while solving a continuous problem  $\mathbf{R}$ , whose size can be effectively controlled through proper constraint management between iterations.

To summarize, for problems of manageable size, where solving the MILP master/sub problem or generating valid inequalities for the original formulation on a per-scenario basis remains computationally efficient, the aforementioned oracles can be more effective than disjunctive Benders decomposition. However, *the key advantage of disjunctive Benders decomposition lies in its scalability for very large problems, achieved by strategically leveraging simple, typical oracles*.

## 5 Numerical experiments

As discussed in Section 4, the key advantage of disjunctive Benders decomposition lies in its ability to tackle large problems by strategically leveraging simple, typical oracles. To demonstrate this, we evaluate the proposed method on large-scale instances of the uncapacitated facility location problem (**UFLP**) and the stochastic network interdiction problem (**SNIP**)—each presenting distinct structural features, which we describe in detail later. Formal problem formulations are provided in Appendix B. We assess computational performance through a comparative analysis with conventional Benders decomposition, augmented with structure-exploiting **TYPICALORACLES**, as well as an off-the-shelf solver.

## 5.1 Datasets

**UFLP** We utilize the **KG** instances from [24] and [21]. The benchmark comprises 90 problem instances, each with an equal number of customers and potential facilities from  $\{250, 500, 750\}$ . For each problem size, there are two main classes: symmetric instances (denoted **gs**) and asymmetric instances (denoted **ga**). Within each class, there are three subclasses—**a**, **b**, and **c**—which differ in their cost configurations. Specifically, in subclass **a**, transportation costs dominate, being an order of magnitude larger than facility opening costs; in subclass **b**, both cost components are of similar magnitude; in subclass **c**, facility opening costs dominate, exceeding allocation costs by an order of magnitude.

**SNIP** We use the **snipno3** and **snipno4** test sets, each consisting of five base instances, originally introduced by [29] and subsequently used in [10, 22]. These instances are obtained from the online companion of [22]. Each instance comprises 456 scenarios and 320 binary first-stage decision variables, and all share a common network topology with 783 nodes and 2,586 arcs. The **snipno3** and **snipno4** instances differ in the probability of undetected traversal when a sensor is not installed. In **snipno3**, the probability of traversing a link undetected without a sensor is 0.1 times that with a sensor, whereas in **snipno4**, it is 0. For each base instance, the sensor installation budget  $b$  varies from 30.0 to 90.0 in increments of 10, resulting in 70 total instances.

## 5.2 Baseline Algorithms

- **EXT**: For all problem instances, we include the extensive formulation (MILP) as a baseline, solved using an off-the-shelf solver.
- **CBD**: As another baseline, we implement conventional BENDERSBNB for each problem, where a TYPICALORACLE is invoked via a lazy constraint callback whenever an incumbent solution is identified. For **UFLP**, we use the solver-free TYPICALORACLE proposed in [16], which exploits the separable structure of the subproblem: once the facility opening decision  $x$  is fixed as  $\hat{x}$ , **sub**( $\hat{x}$ ) decomposes into independent continuous knapsack problems—one per customer—with closed-form solutions. We adopt the fat version of the method, where individual Benders cuts are generated for each violated customer constraint, which outperforms the slim (aggregated cut) version.

For **SNIP**, we use the conventional TYPICALORACLE, in which the subproblem (**sub**( $\hat{x}$ )) is decomposed by scenario and solved via an off-the-shelf solver.

- **DBD**: For each problem, we implement disjunctive BENDERSBNB, incorporating the same lazy constraint callback used in **CBD**, along with an additional user callback. This user callback is equipped with THE ORACLE (Routine 1) or its approximate version (Routine 4), both of which internally leverage the same TYPICALORACLE used in the lazy callback. The user callback invokes THE ORACLE (or its approximation) periodically—every 500 fractional nodes—for both **UFLP** and **SNIP**.

For both CBD and DBD, one could opt to add Benders cuts as user cuts via `TYPICALORACLES` at each fractional node, up to a specified number of visits, as done in [16]. However, in our experiment, we omit such user cuts in both CBD and DBD, as we observed that they significantly increase computation time on certain easy **UFLP** instances. Furthermore, since the primary objective of this paper is to evaluate the strength of cutting planes, we intentionally refrain from using advanced heuristics or solver strategies beyond those implemented through custom cut callback functions, even if such enhancements were considered in prior studies.

### 5.2.1 Implementation details

All implementations were developed in Julia, using JuMP’s solver-independent callback framework, and all optimization models were solved using IBM ILOG CPLEX 22.1.1.0 through the JuMP modeling interface. All computational experiments were conducted on a Linux system equipped with two Intel Xeon Gold 6330 CPUs @ 2.00 GHz, each with 56 cores. We executed 8 experiments in parallel, allocating 60 GB of memory and 7 CPU cores to each, with a time limit of 4 hours per experiment. The source code is publicly available at <https://github.com/asu-opt-lab/BendersDecomposition.git>.

**CPLEX parameter settings** For `EXT`, we primarily use the default CPLEX parameters, with the following modifications to restrict the solver to a fixed number of threads and to enhance numerical precision: `CPX_PARAM_THREADS` = 7, `CPX_PARAM_EPINT` =  $10^{-9}$ , `CPX_PARAM_EPRHS` =  $10^{-9}$ , and `CPX_PARAM_EPGAP` =  $10^{-6}$ . For both CBD and DBD, we apply the same parameter settings to the master problem as in `EXT`, except for the thread parameter: when using callbacks, CPLEX automatically restricts execution to a single thread. Additionally, for **UFLP**, we set `CPX_PARAM_BRDIR` = 1 to prioritize branching in the upward direction, following [16]; this setting is applied to `EXT` and to the master problems of both CBD and DBD. For solving `R` (a relaxation of `(DCGLP)`) and `sub`( $\hat{x}$ ) for solver-based `TYPICALORACLES`, we use default solver parameters, except for the following adjustments to enhance numerical stability and solution accuracy: `CPX_PARAM_THREADS` = 7, `CPX_PARAM_EPRHS` =  $10^{-9}$ , `CPX_PARAM_EPOPT` =  $10^{-9}$ , and `CPX_PARAM_NUMERICALEMPHASIS` = 1.

**Root node processing** For all `BENDERSBNB` variants, we begin by solving the LP relaxation of (1.1) at the root node using `BENDERSSSEQ` equipped with the `TYPICALORACLES` described earlier. For **UFLP** and **SNIP**, the LP relaxations of all instances are solved to a tolerance of  $10^{-9}$  within 10 seconds and 80 seconds, respectively.

**THE (APPROX)ORACLE configurations** For all problems, we use simple split of the form  $(\phi, \phi_0) = (e_i, 0)$  for some  $i \in [\ell]$ , constructed using the variable with the largest fractional value. The generated lift-and-project cuts are strengthened via (3.1) before being added to the master problem, and all previously generated disjunctive cuts are included in `(DCGLP)` (see Remark 6). We set  $p = \infty$  and terminate THE (APPROX)ORACLE either when the optimality gap falls below  $10^{-3}$ ,

or earlier if the lower bound fails to improve over three consecutive iterations. In addition, we tailor the configuration of THE (APPROX)ORACLE to the specific characteristics of each problem. For **UFLP**, the solver-free TYPICALORACLE is computationally cheap but often yields a large number of cuts, which can hinder the performance of the master problem’s branch-and-bound process. To prioritize cut quality and incorporate cuts selectively, we add only the top 5% of the most violated byproduct Benders cuts to the master problem, and we do not reuse the relaxation  $R$ —that is, all byproduct Benders cuts generated in earlier disjunctive cut generation are discarded from  $R$ . Lifting is disabled, meaning THE ORACLE is used in its non-approximated form. For **SNIP**, the TYPICALORACLE is more computationally intensive as it solves 456 solver-based subproblems, and it does not benefit from parallelization in our implementation. To reduce the frequency of solving  $\text{sub}(\hat{x})$ , we reuse the relaxation  $R$ , add all violated byproduct Benders cuts to the master problem, and employ THE APPROXORACLE as described in Routine 4.

### 5.3 UFLP

Table 1 presents benchmark results for 33 **KG** instances that are solved optimally by **DBD** within the 4-hour time limit. The metrics compared include node count (NC) and runtime in seconds (Time). Across the 33 instances, **DBD** consistently outperforms both **EXT** and **CBD** in terms of runtime. Notably, **EXT** fails to solve 14 out of 30 instances within the time limit. While **CBD** performs better—successfully solving 26 instances—it still lags behind **DBD**, especially on computationally nontrivial instances (i.e., those requiring more than 150 seconds). In contrast, **DBD** solves all 30 instances within the time limit and achieves the lowest runtime on all nontrivial cases. Especially, for large-scale instances in **ga500/gs500**, both **EXT** and **CBD** fail to complete within 4 hours, whereas **DBD** successfully solves them in around 13,000 seconds.

Column  $\frac{(3)}{(1)}$  reports the ratio of node counts between **DBD** and **CBD**, with values ranging from 0.09 to 1.10 and a mean of approximately 0.26. This indicates that, on average, **DBD** explores about four times fewer nodes than **CBD**. The performance advantage of **DBD** is especially pronounced for the six instances that require more than one hour for **CBD** to solve to optimality (**a-3**, **a-5**, **b-1**, **b-3**, **b-4** under **ga250**, and **b-3** under **gs250**); for these instances, the average node count ratio drops to 13.33%. *Remarkably, DBD achieves a node count comparable to—or even smaller than—that of EXT for nontrivial instances of types a and b, despite operating in a decomposed formulation.* This is surprising, as one would expect **EXT**, which retains the full problem information, to yield the smallest branch-and-bound tree. Indeed, **CBD** requires exploring an order of magnitude more nodes than **EXT** due to information loss from decomposition, and the smaller runtime is because the computational savings from solving modular problems outweigh the additional search overhead. In contrast, **DBD** goes further by recovering node counts comparable to **EXT** while retaining the computational benefits of decomposition. This observation suggests that **DBD** effectively preserves the strength of the original formulation, while simultaneously exploiting the modularity and efficiency of a decomposed approach.

For the remaining 57 **KG** instances that are not solved to optimality by all approaches within the

Table 1: Benchmark results for KG instances solved optimally by DBD: EXT vs. CBD vs. DBD

Instance	EXT		CBD		DBD		Summary	
	Node Count (NC)	Time	NC (1)	Time (2)	NC (3)	Time (4)	$\frac{(3)}{(1)}$	$\mathbb{I}[(2) > (4)]$
<b>ga250</b>								
a-1	33,640	2,305.23	175,553	741.66	45,944	370.74	0.26	1
a-2	5,652	350.50	18,076	101.13	9,662	79.69	0.53	1
a-3	142,939	9,435.19	1,467,854	6,419.34	133,940	1,396.96	0.09	1
a-4	43,379	3,160.07	233,059	1,278.27	54,586	515.25	0.23	1
a-5	149,060	12,206.09	1,132,672	4,976.77	193,964	2,181.83	0.17	1
b-1	42,958	†	980,907	4,846.27	176,770	2,511.40	0.18	1
b-2	20,047	7,907.71	282,139	1,144.45	87,039	737.18	0.31	1
b-3	35,752	†	993,537	5,528.37	134,410	1,909.06	0.14	1
b-4	46,086	†	1,291,540	6,360.08	152,981	2,364.46	0.12	1
b-5	31,192	†	410,728	2,449.24	122,864	1,643.13	0.30	1
c-1	1,645	2,694.43	7,869	57.69	8,015	74.43	1.02	0
c-2	625	1,670.30	5,959	33.81	6,297	53.59	1.06	0
c-3	1,283	2,344.44	8,063	55.79	7,141	71.16	0.89	0
c-4	869	1,777.30	7,277	38.87	6,316	63.71	0.87	0
c-5	1,152	1,949.82	7,776	51.63	6,229	61.72	0.80	0
<b>gs250</b>								
a-1	21,754	1,291.54	139,342	643.41	31,522	215.50	0.23	1
a-2	4,248	345.26	24,657	161.47	12,869	120.26	0.52	1
a-3	69,805	4,087.00	266,509	1,131.92	59,321	426.79	0.22	1
a-4	40,706	4,074.93	228,880	1,083.48	63,313	550.08	0.28	1
a-5	51,196	3,278.57	247,966	1,029.96	57,971	540.26	0.23	1
b-1	28,537	†	2,354,995	†	362,479	9,729.54	0.15	1
b-2	31,974	†	444,039	2,144.95	92,772	1,034.79	0.21	1
b-3	29,787	†	1,402,121	6,423.72	146,065	2,040.72	0.10	1
b-4	22,735	10,111.28	378,571	2,055.20	84,702	960.54	0.22	1
b-5	28,862	†	365,434	1,755.69	75,742	881.78	0.21	1
c-1	853	1,439.28	7,465	52.89	5,940	65.16	0.80	0
c-2	1,956	2,254.64	9,668	62.07	10,654	84.85	1.10	0
c-3	1,239	1,905.05	9,039	59.28	7,379	75.25	0.82	0
c-4	847	1,117.43	6,025	46.34	6,618	60.55	1.10	0
c-5	2,667	2,113.01	11,590	118.53	9,674	120.79	0.83	0
<b>ga500</b>								
c-1	1,211	†	447,006	†	154,942	10,508.10	0.35	1
<b>gs500</b>								
c-1	1,146	†	559,468	†	198,236	13,185.10	0.35	1
c-2	1,115	†	717,632	†	178,469	13,381.00	0.25	1

† Reached the 4-hour time limit.

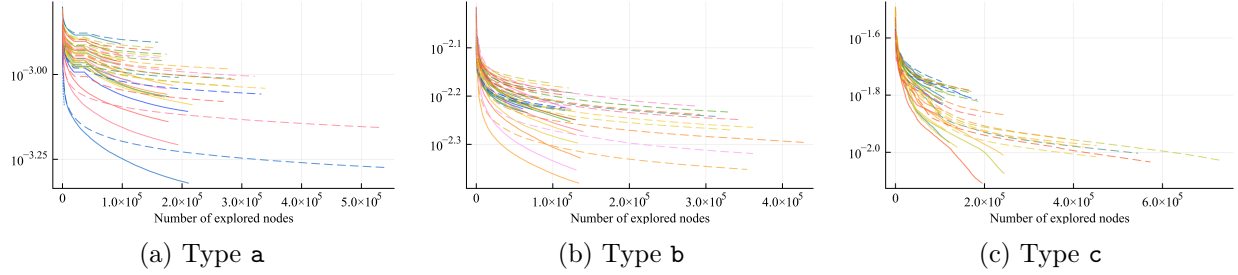


Figure 5: Progress of gap (%) to best known upper bounds: EXT (dotted) vs. CBD (dashed) vs. DBD (solid)

time limit, we compare the lower bounds and the number of explored nodes to assess the strength of the generated cuts. We intentionally exclude upper bound comparisons, as they are more sensitive to heuristic variations and less indicative of cut quality. Figure 5 illustrates the progress of the optimality gap (relative to the best-known upper bound reported in [16]) as a function of the number of explored nodes. Each color represents a different instance. Solid lines trace the progress of DBD, while dashed lines correspond to CBD. The progress of EXT is also shown using dotted lines, which are mostly concentrated on the left side of the plot—reflecting the significantly smaller number of nodes it explores; this behavior highlights the difficulty of the instances and underscores the limited scalability of EXT.

The figure reveals a clear tail-off effect for CBD, which makes rapid initial improvements but then stagnates for extended periods. In contrast, DBD is less affected by this phenomenon; its gap progression curves are generally steeper and less flat than those of CBD, indicating more consistent improvement over time. In 46 out of the 57 instances (approximately 80% of the unsolved **UFLP** instances), DBD achieves a higher final lower bound than CBD. In the remaining 20% of the unsolved instances, DBD produces a lower lower bound, as it explores fewer nodes within the same time limit. This is primarily due to two factors: (i) the computational overhead associated with generating disjunctive Benders cuts, and (ii) the additional burden of managing a large number of byproduct cuts added to the master problem. These observations suggest that the performance of DBD could be further improved by accelerating the disjunctive cut generation process—e.g., via bundle-type methods—and by employing more effective strategies for constraint management.

#### 5.4 SNIP

For all **snipno3** and **snipno4** instances, EXT fails to reach optimality within the 4-hour time limit. However, both test sets are considered relatively easy under the BD framework, as CBD solves all 70 instances with an average runtime of 194.41 seconds. Only one case—Instance 1 in **snipno3** with budget 90—takes longer than 15 minutes, terminating after 1,274.76 seconds. Since CBD is already highly efficient on these instances, the additional cost of solving all 456 subproblems multiple times (without parallelization) to generate disjunctive cuts is not offset. As a result, DBD incurs greater computational overhead: on average, it requires 2.30 times more runtime than CBD for **snipno3**, and

1.81 times more for `snipno4`, despite exploring only about 79% as many nodes as `CBD`.

Nonetheless, our results show that `DBD` can outperform `CBD` in both runtime and node count particularly in instances where `CBD` struggles. In the most difficult case—Instance 1 of `snipno3` with budget 90—`DBD` solves the problem approximately 100 seconds faster than `CBD`, despite the substantial overhead from sequential subproblem solves. This advantage stems from the significant reduction in the final branch-and-bound tree: `DBD` explores only 16% of the nodes required by `CBD`. To further investigate, we conducted additional experiments with budget values ranging from 100 to 150. We identified Instance 1 with budget 90, and Instances 0 and 1 with budget 140 in `snipno3` as the most challenging. For these instances, `CBD` requires an average of 1,764.14 seconds, while `DBD` completes them in just 79.2% of that time—even though it solves decomposed subproblems sequentially. Moreover, the average node count ratio across these instances is only 10.1%, highlighting the substantial improvement in node efficiency.

To summarize, our experiments on `SNIP` align with the conclusions of [10]: as instances become easier, the cost of repeatedly solving subproblems (without parallelization) may outweigh the benefits of stronger cuts. However, the results indicate that `DBD` remains particularly effective for difficult instances, demonstrating its scalability, and its performance can be further enhanced through parallel computing or scenario sampling strategies.

## 6 Conclusions

This paper introduced disjunctive Benders decomposition (`DBD`), a novel enhancement of classic `BD`, which integrates disjunctive programming theory to generate stronger cuts valid for the convex hull of the Benders reformulation. Unlike conventional `BD`—which typically produces cuts tight only for the continuous relaxation—our approach explicitly incorporates integrality information into the cut-generation process. Specifically, we developed both exact and approximate variants of a disjunctive cut-generating oracle for the Benders reformulation that can operate on top of any existing typical Benders oracles. The proposed disjunctive oracles construct valid inequalities via iterative separation in an extended space, without introducing additional integer variables into the subproblem. We also extended standard strengthening and lifting techniques—originally developed for disjunctive cuts based on simple binary-variable splits—into the `BD` framework. These enhancements improve cut quality and reduce the computational burden of the proposed oracles while ensuring their validity throughout the entire branch-and-bound tree. Computational experiments on large-scale instances of uncapacitated facility location (`UFLP`) and stochastic network interdiction (`SNIP`) problems demonstrated advantages of `DBD` empirically. For the `UFLP` instances, `DBD` consistently outperforms both the extensive formulation and conventional `BD`, solving more instances to optimality, reducing node counts by up to a factor of ten, and alleviating the tail-off behavior commonly observed in standard `BD`. Notably, `DBD` retains much of the strength of full-space formulations while exploiting the computational benefits of decomposition, especially on challenging `UFLP` instances. For `SNIP`, while subproblem complexity impacts overall runtime, `DBD` achieves

significantly better node efficiency on harder instances, highlighting its promise for solving large-scale mixed-integer programming problems. In summary, DBD offers a scalable and general-purpose framework for high-performance mixed-integer optimization. Future work includes accelerating oracle execution through bundle-type methods, leveraging parallelism more effectively, and developing adaptive strategies for disjunction selection to further enhance performance.

## References

- [1] Egon Balas. Disjunctive programming. *Annals of discrete mathematics*, 5:3–51, 1979.
- [2] Egon Balas. Disjunctive programming: Properties of the convex hull of feasible points. *Discrete Applied Mathematics*, 89(1-3):3–44, 1998.
- [3] Egon Balas. *Disjunctive programming*. Springer, 2018.
- [4] Egon Balas, Sebastián Ceria, and Gérard Cornuéjols. A lift-and-project cutting plane algorithm for mixed 0–1 programs. *Mathematical programming*, 58(1-3):295–324, 1993.
- [5] Egon Balas, Sebastián Ceria, and Gérard Cornuéjols. Mixed 0-1 programming by lift-and-project in a branch-and-cut framework. *Management Science*, 42(9):1229–1246, 1996.
- [6] Egon Balas and Michael Perregaard. Lift-and-project for mixed 0–1 programming: recent progress. *Discrete Applied Mathematics*, 123(1-3):129–154, 2002.
- [7] Walid Ben-Ameur and José Neto. Acceleration of cutting-plane and column generation algorithms: Applications to network design. *Networks: An International Journal*, 49(1):3–17, 2007.
- [8] Dimitri Bertsekas. *Convex optimization theory*, volume 1. Athena Scientific, 2009.
- [9] Dimitri P Bertsekas. Nonlinear programming. *Journal of the Operational Research Society*, 48(3):334–334, 1997.
- [10] Merve Bodur, Sanjeeb Dash, Oktay Günlük, and James Luedtke. Strengthened benders cuts for stochastic integer programs with continuous recourse. *INFORMS Journal on Computing*, 29(1):77–91, 2017.
- [11] Merve Bodur and James R Luedtke. Mixed-integer rounding enhanced benders decomposition for multiclass service-system staffing and scheduling with arrival rate uncertainty. *Management Science*, 63(7):2073–2091, 2017.
- [12] Geunyeong Byeon and Pascal Van Hentenryck. Benders subproblem decomposition for bilevel problems with convex follower. *INFORMS Journal on Computing*, 34(3):1749–1767, 2022.
- [13] Michele Conforti, Gérard Cornuéjols, and Giacomo Zambelli. *Integer programming*. Springer, 2014.

- [14] William Cook, Ravindran Kannan, and Alexander Schrijver. Chvátal closures for mixed integer programming problems. *Mathematical Programming*, 47(1):155–174, 1990.
- [15] Arnaud Deza and Elias B Khalil. Machine learning for cutting planes in integer programming: A survey. *arXiv preprint arXiv:2302.09166*, 2023.
- [16] Matteo Fischetti, Ivana Ljubić, and Markus Sinnl. Redesigning benders decomposition for large-scale facility location. *Management Science*, 63(7):2146–2162, 2017.
- [17] Matteo Fischetti, Andrea Lodi, and Andrea Tramontani. On the separation of disjunctive cuts. *Mathematical Programming*, 128(1-2):205–230, 2011.
- [18] Matteo Fischetti, Domenico Salvagnin, and Arrigo Zanette. A note on the selection of benders' cuts. *Mathematical Programming*, 124:175–182, 2010.
- [19] Bernard Fortz and Michael Poss. An improved benders decomposition applied to a multi-layer network design problem. *Operations research letters*, 37(5):359–364, 2009.
- [20] Dinakar Gade, Simge Küçükyavuz, and Suvrajeet Sen. Decomposition algorithms with parametric gomory cuts for two-stage stochastic integer programs. *Mathematical Programming*, 144(1-2):39–64, 2014.
- [21] Diptesh Ghosh. Neighborhood search heuristics for the uncapacitated facility location problem. *European Journal of Operational Research*, 150(1):150–162, 2003.
- [22] Mojtaba Hosseini and John Turner. Deepest cuts for benders decomposition. *Operations Research*, 2024.
- [23] Huiwen Jia and Siqian Shen. Benders cut classification via support vector machines for solving two-stage stochastic programs. *INFORMS Journal on Optimization*, 3(3):278–297, 2021.
- [24] Manfred Körkel. On the exact solution of large-scale simple plant location problems. *European Journal of Operational Research*, 39(2):157–173, 1989.
- [25] Andrea Lodi, Mathieu Tanneau, and Juan-Pablo Vielma. Disjunctive cuts in mixed-integer conic optimization. *Mathematical Programming*, 199(1):671–719, 2023.
- [26] Thomas L Magnanti and Richard T Wong. Accelerating benders decomposition: Algorithmic enhancement and model selection criteria. *Operations research*, 29(3):464–484, 1981.
- [27] Stephen J Maher. Implementing the branch-and-cut approach for a general purpose benders' decomposition framework. *European Journal of Operational Research*, 290(2):479–498, 2021.
- [28] Joe Naoum-Sawaya and Samir Elhedhli. An interior-point benders based branch-and-cut algorithm for mixed integer programs. *Annals of Operations Research*, 210:33–55, 2013.

- [29] Feng Pan and David P Morton. Minimizing a stochastic maximum-reliability path. *Networks: An International Journal*, 52(3):111–119, 2008.
- [30] Nikolaos Papadakos. Practical enhancements to the magnanti–wong method. *Operations Research Letters*, 36(4):444–449, 2008.
- [31] Ragheb Rahmaniani, Shabbir Ahmed, Teodor Gabriel Crainic, Michel Gendreau, and Walter Rei. The benders dual decomposition method. *Operations Research*, 68(3):878–895, 2020.
- [32] Ragheb Rahmaniani, Teodor Gabriel Crainic, Michel Gendreau, and Walter Rei. The benders decomposition algorithm: A literature review. *European Journal of Operational Research*, 259(3):801–817, 2017.
- [33] Suvrajeet Sen and Julia L Higle. The c 3 theorem and a d 2 algorithm for large scale stochastic mixed-integer programming: Set convexification. *Mathematical Programming*, 104:1–20, 2005.
- [34] Kiho Seo, Seulgi Joung, Chungmok Lee, and Sungsoo Park. A closest benders cut selection scheme for accelerating the benders decomposition algorithm. *INFORMS Journal on Computing*, 34(5):2804–2827, 2022.
- [35] Jikai Zou, Shabbir Ahmed, and Xu Andy Sun. Stochastic dual dynamic integer programming. *Mathematical Programming*, 175:461–502, 2019.

## Appendix A Omitted proofs

### A.1 Proof of Lemma 1

It is easy to verify that (DCGLP) is a strong dual to (CGLP), as the weak form of Slater's condition is met with  $\mathbf{0}$  serving as a Slater point for (CGLP). In addition, it is well-known that  $\text{conv}(\mathcal{P}^{(\phi, \phi_0)})$  is a polyhedron, and its representation is given by (see, e.g., [13, Lemma 4.45])

$$\text{conv}(\mathcal{P}^{(\phi, \phi_0)}) = \{(\kappa_x + \nu_x, \kappa_t + \nu_t) : (\text{DCGLP.b}) - (\text{DCGLP.i})\}.$$

This equivalence is not hard to verify: for any  $(\kappa_x, \kappa_t, \kappa_0, \nu_x, \nu_t, \nu_0)$  satisfying (DCGLP.b)-(DCGLP.i), and using the convention that  $0 \times \infty = 0$ , we have

$$(\kappa_x + \nu_x, \kappa_t + \nu_t) = \kappa_0(\kappa_x/\kappa_0, \kappa_t/\kappa_0) + \nu_0(\nu_x/\nu_0, \nu_t/\nu_0) \in \text{conv}(\mathcal{P}^{(\phi, \phi_0)}),$$

because (i) when  $\kappa_0 > 0$ ,  $(\kappa_x/\kappa_0, \kappa_t/\kappa_0) \in \mathcal{P}_1^{(\phi, \phi_0)}$ ; (ii) when  $\nu_0 > 0$ ,  $(\nu_x/\nu_0, \nu_t/\nu_0) \in \mathcal{P}_2^{(\phi, \phi_0)}$ ; and (iii)  $\kappa_0 + \nu_0 = 1$ . Thus,  $\text{conv}(\mathcal{P}^{(\phi, \phi_0)}) \supseteq \{(\kappa_x + \nu_x, \kappa_t + \nu_t) : (\text{DCGLP.b}) - (\text{DCGLP.i})\}$ , and for  $\text{conv}(\mathcal{P}^{(\phi, \phi_0)}) = \emptyset$ , the equivalence follows trivially. Conversely, when  $\text{conv}(\mathcal{P}^{(\phi, \phi_0)}) \neq \emptyset$ , for any  $(x, t) \in \text{conv}(\mathcal{P}^{(\phi, \phi_0)})$ , there exist  $(x_1, t_1) \in \mathcal{P}_1^{(\phi, \phi_0)}$ ,  $(x_2, t_2) \in \mathcal{P}_2^{(\phi, \phi_0)}$  (or at least one of these if the other polyhedron is empty), and  $\lambda \in [0, 1]$  such that  $(x, t) = \lambda(x_1, t_1) + (1 - \lambda)(x_2, t_2)$ . By setting  $(\kappa_x, \kappa_t, \kappa_0, \nu_x, \nu_t, \nu_0) = (\lambda x_1, \lambda t_1, \lambda, (1 - \lambda)x_2, (1 - \lambda)t_2, 1 - \lambda)$ , we can verify that this satisfies (DCGLP.b)-(DCGLP.i).

By replacing (DCGLP.b)-(DCGLP.i) with the equivalent condition  $(\kappa_x + \nu_x, \kappa_t + \nu_t) \in \text{conv}(\mathcal{P}^{(\phi, \phi_0)})$ , eliminating the auxiliary variables  $s_x$ ,  $s_t$ , and  $\tau$ , and applying the variable substitution  $(x, t) = (\kappa_x + \nu_x, \kappa_t + \nu_t)$ , we obtain (2.4), which represents the projection problem.  $\square$

### A.2 Proof of Proposition 1

When (MILP) is feasible, i.e.,  $\text{conv}((\mathcal{X} \times \mathbb{R}) \cap \mathcal{L}) \neq \emptyset$ , then  $\text{conv}(\mathcal{P}^{(\phi, \phi_0)})$  is nonempty, closed, and convex. This holds because  $\text{conv}((\mathcal{X} \times \mathbb{R}) \cap \mathcal{L}) \subseteq \text{conv}(\mathcal{P}^{(\phi, \phi_0)})$ , and the latter is a polyhedron (see, e.g., Lemma 1). Consequently, by the projection theorem, (2.4) always attains a finite, nonnegative optimal value, which is zero if and only if  $(\hat{x}, \hat{t}) \in \text{conv}(\mathcal{P}^{(\phi, \phi_0)})$ . Furthermore, when  $p = 2$ , the strong convexity of the squared objective function ensures the uniqueness of the optimum (see, e.g., [9, Proposition 1.1.4]).

Let  $(\hat{\kappa}, \hat{\nu}, \hat{s}, \hat{\tau})$  be an optimal solution of (DCGLP). We show that  $\hat{\gamma}_x^\top(\hat{\kappa}_x + \hat{\nu}_x) + \hat{\gamma}_t(\hat{\kappa}_t + \hat{\nu}_t) - \hat{\gamma}_0 = 0$ , which implies that the valid inequality  $\hat{\gamma}_0 - \hat{\gamma}_x^\top x - \hat{\gamma}_t^\top t \leq 0$  meets  $\text{conv}(\mathcal{P}^{(\phi, \phi_0)})$  at  $(x', t') = (\hat{\kappa}_x + \hat{\nu}_x, \hat{\kappa}_t + \hat{\nu}_t) \in \text{conv}(\mathcal{P}^{(\phi, \phi_0)})$ . Note that

$$\begin{aligned} \hat{\gamma}_0 - \hat{\gamma}_x^\top \hat{x} - \hat{\gamma}_t^\top \hat{t} &= \|(\hat{s}_x, \hat{s}_t)\|_p + \hat{\gamma}_x^\top(\hat{\kappa}_x + \hat{\nu}_x - \hat{x} - \hat{s}_x) + \hat{\gamma}_t(\hat{\kappa}_t + \hat{\nu}_t - \hat{t} - \hat{s}_t) \\ &\geq \min_{(s_x, s_t) \in \mathbb{R}^{n_x+1}} \|(\hat{s}_x, \hat{s}_t)\|_p + \hat{\gamma}_x^\top(\hat{\kappa}_x + \hat{\nu}_x - \hat{x} - s_x) + \hat{\gamma}_t(\hat{\kappa}_t + \hat{\nu}_t - \hat{t} - s_t) \\ &= -\hat{\gamma}_0 + \hat{\gamma}_x^\top(\hat{\kappa}_x + \hat{\nu}_x) + \hat{\gamma}_t(\hat{\kappa}_t + \hat{\nu}_t) + \hat{\gamma}_0 - \hat{\gamma}_x^\top \hat{x} - \hat{\gamma}_t^\top \hat{t}, \end{aligned}$$

where the first equality follows from the strong duality of (DCGLP) and the feasibility of  $(\hat{\kappa}, \hat{\nu}, \hat{s}, \hat{\tau})$  to (DCGLP), the inequality results from partially minimizing over  $s$ , and the final equality uses the conjugate of the  $l_p$ -norm and the feasibility of  $\hat{\gamma}$  to (CGLP), i.e.,  $\|(\hat{\gamma}_x, \hat{\gamma}_t)\|_q \leq 1$ .

This yields

$$-\hat{\gamma}_0 + \hat{\gamma}_x^\top (\hat{\kappa}_x + \hat{\nu}_x) + \hat{\gamma}_t^\top (\hat{\kappa}_t + \hat{\nu}_t) \leq 0,$$

and the reverse inequality follows from the validity of  $\hat{\gamma}_0 - \hat{\gamma}_x^\top x - \hat{\gamma}_t^\top t \leq 0$  for  $\text{conv}(\mathcal{P}^{(\phi, \phi_0)})$  and  $(\hat{\kappa}_x + \hat{\nu}_x, \hat{\kappa}_t + \hat{\nu}_t) \in \text{conv}(\mathcal{P}^{(\phi, \phi_0)})$ , implying that the inequality must hold with equality.  $\square$

### A.3 Proof of Proposition 2

Consider the optimization problem  $\min \alpha_x^\top \omega_x + \alpha_t \omega_t - \alpha_0 \omega_0 : (\omega_x, \omega_t, \omega_0) \in \mathcal{L}^\#$  which can be rewritten as follows, where the variables in parentheses indicate their associated dual variables:

$$\begin{aligned} & \min \alpha_x^\top \omega_x + \alpha_t \omega_t - \alpha_0 \omega_0 \\ (\lambda_{\hat{\pi}}) \quad & \text{s.t. } \omega_t \geq \hat{\pi}^\top (b\omega_0 - A\omega_x), \quad \forall \hat{\pi} \in \mathcal{J}, \\ (\mu_{\tilde{\pi}}) \quad & 0 \geq \tilde{\pi}^\top (b\omega_0 - A\omega_x), \quad \forall \tilde{\pi} \in \mathcal{R}, \\ & \omega_0 \geq 0 \end{aligned}$$

The dual of this problem is a feasibility problem:

$$\begin{aligned} & \max 0 \\ \text{s.t. } & \sum_{\hat{\pi} \in \mathcal{J}} \lambda_{\hat{\pi}} = \alpha_t, \\ & \sum_{\hat{\pi} \in \mathcal{J}} \lambda_{\hat{\pi}} A^\top \hat{\pi} + \sum_{\tilde{\pi} \in \mathcal{R}} \mu_{\tilde{\pi}} A^\top \tilde{\pi} = \alpha_x, \\ & \sum_{\hat{\pi} \in \mathcal{J}} \lambda_{\hat{\pi}} b^\top \hat{\pi} + \sum_{\tilde{\pi} \in \mathcal{R}} \mu_{\tilde{\pi}} b^\top \tilde{\pi} \geq \alpha_0, \\ & ((\lambda_{\hat{\pi}})_{\hat{\pi} \in \mathcal{J}}, (\mu_{\tilde{\pi}})_{\tilde{\pi} \in \mathcal{R}}) \geq 0. \end{aligned}$$

Since  $\alpha_x^\top x + \alpha_t t \geq \alpha_0$  is a valid inequality for  $\mathcal{L} = \{(x, t) \in \mathbb{R}^{n_x+1} : (1.1b), (1.1c)\}$ , there exist corresponding Farkas multipliers  $((\lambda_{\hat{\pi}})_{\hat{\pi} \in \mathcal{J}}, (\mu_{\tilde{\pi}})_{\tilde{\pi} \in \mathcal{R}}) \geq 0$  satisfying  $\alpha_x = \sum_{\hat{\pi} \in \mathcal{J}} \lambda_{\hat{\pi}} A^\top \hat{\pi} + \sum_{\tilde{\pi} \in \mathcal{R}} \mu_{\tilde{\pi}} A^\top \tilde{\pi}$ ,  $\alpha_t = \sum_{\hat{\pi} \in \mathcal{J}} \lambda_{\hat{\pi}}$ , and  $\alpha_0 \leq \sum_{\hat{\pi} \in \mathcal{J}} \lambda_{\hat{\pi}} b^\top \hat{\pi} + \sum_{\tilde{\pi} \in \mathcal{R}} \mu_{\tilde{\pi}} b^\top \tilde{\pi}$ . This establishes the feasibility of the dual problem, implying that the optimal objective value of the primal problem is zero. Therefore, for all  $(\omega_x, \omega_t, \omega_0) \in \mathcal{L}^\#$ ,  $\alpha_x^\top \omega_x + \alpha_t \omega_t - \alpha_0 \omega_0 \geq 0$ , confirming that the inequality is valid for  $\mathcal{L}^\#$ . Moreover, the inequality separates  $(\hat{\omega}_x, \hat{\omega}_t, \hat{\omega}_0)$  because  $0 > \alpha_x^\top x' + \alpha_t t' - \alpha_0 = \alpha_x^\top (\hat{\omega}_x / \hat{\omega}_0) + \alpha_t (\hat{\omega}_t / \hat{\omega}_0) - \alpha_0$  and  $\hat{\omega}_0 > 0$ . Furthermore, it follows directly that if  $(x', t') = (\hat{\omega}_x / \hat{\omega}_0, \hat{\omega}_t / \hat{\omega}_0) \in \mathcal{L}$ , then  $(\hat{\omega}_x, \hat{\omega}_t, \hat{\omega}_0) \in \mathcal{L}^\#$  by multiplying all the constraints in  $\mathcal{L}$  with  $\hat{\omega}_0 > 0$ .  $\square$

## A.4 Proof of Proposition 3

$\mathbb{R}^{(\rho)}$  corresponds to (DCGLP) with the polyhedral set  $\mathcal{L}$  replaced by its polyhedral relaxation  $\mathcal{L}^{(\rho)}$ . Thus, the statements follow directly from Lemma 1 and Proposition 1.  $\square$

## A.5 Proof of Theorem 1

By design, Lines 8-12 in Algorithm 3 are executed only when  $(\hat{x}, \hat{t})$  is an optimal basic solution of

$$\min\{c^\top x + t : (x, t) \in \mathcal{L}, x \in \mathcal{X}_{LP}, (x, t) \in \mathcal{D}\}, \quad (\text{A.1})$$

where  $\mathcal{D}$  is the polyhedron defined by the disjunctive cuts found up to that point. Accordingly, Algorithm 3 can be viewed as a variant of the specialized, finitely convergent lift-and-project algorithm originally proposed in [4] for solving

$$\min\{c^\top x + t : (x, t) \in \mathcal{L}, x \in \mathcal{X}\}.$$

The key differences are twofold: first, the use of standard Benders decomposition to compute an optimal basic solution at each outer iteration  $k$ ; and second, the adoption of  $\gamma$ -normalization in the disjunctive cut separation problem, in place of the standard normalization used in [4]. It is well known that the standard Benders decomposition is finitely convergent for each instance of (A.1) updated with a newly added disjunctive cut. Moreover, the disjunctive cut generated at Line 12 always cuts off the current solution  $(x^{(k)}, t^{(k)})$ , and only finitely many such cuts can be produced overall. This follows from the fact that the finite convergence proof for the original lift-and-project method—given in [4, Theorem 3.1] and [13, Theorem 5.24]—extends naturally to the case of  $\gamma$ -normalization with  $l_1$ - and  $l_\infty$ -norms. Indeed, the disjunctive cut separation problem remains a linear program with finitely many extreme points, and each disjunctive cut corresponds to one such extreme point. Therefore, the overall algorithm is guaranteed to converge in a finite number of iterations.  $\square$

## A.6 Proof of Proposition 4

Consider a split  $(\phi', \phi'_0) = (e_i - m, 0)$  for some integral vector  $m \in \mathbb{Z}^{n_x}$  with  $m_j = 0$  for  $j \notin \mathcal{I}$ :

$$x_i - m^\top x \leq 0 \vee x_i - m^\top x \geq 1.$$

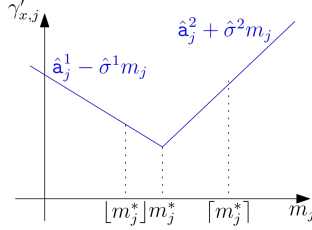


Figure 6: The graph of  $\gamma'_{x,j}$  as a function of  $m_j$ .

Note that since  $l_j = 0$  for  $j \in \mathcal{I}$ ,  $\delta_j^1$  and  $\delta_j^2$  serve as slack variables in (2.1c) and (2.1d), respectively, for  $j \in \mathcal{I}$ . Therefore, we can construct a valid cut  $\gamma'_0 - (\gamma'_x)^\top x - \gamma'_t t \leq 0$  for  $\mathcal{P}^{(\phi', \phi'_0)}$  with

$$\begin{cases} \gamma'_0 = \hat{\gamma}_0, \\ \gamma'_{x,j} = \max\{\hat{a}_j^1 - \hat{\sigma}^1 m_j, \hat{a}_j^2 + \hat{\sigma}^2 m_j\}, \forall j \in \mathcal{I}, \\ \gamma'_{x,j} = \hat{\gamma}_{x,j}, \forall j \in [n_x] \setminus \mathcal{I}, \\ \gamma'_t = \hat{\gamma}_t. \end{cases}$$

Note that  $\gamma'_{x,j}$  is a function of  $m_j$ , as illustrated in Figure 6. Since  $x_j \geq 0$  for  $j \in \mathcal{I}$ , the lower the value of the corresponding  $\gamma'_{x,j}$  is, the tighter the cut  $\gamma'_0 - (\gamma'_x)^\top x - \gamma'_t t \leq 0$  is. Thus, we choose the value of  $m_j$  so that  $\gamma'_{x,j} = \max\{\hat{a}_j^1 - \hat{\sigma}^1 m_j, \hat{a}_j^2 + \hat{\sigma}^2 m_j\}$  is minimized for each  $j \in \mathcal{I}$ . Since both  $\hat{\sigma}^1$  and  $\hat{\sigma}^2$  are nonnegative, the  $m_j$ -value that gives the minimum value of  $\gamma'_{x,j}$  is the point where the two affine functions meet (see Figure 6), i.e.,

$$\hat{a}_j^1 - \hat{\sigma}^1 m_j^* = \hat{a}_j^2 + \hat{\sigma}^2 m_j^* \Rightarrow m_j^* = \frac{\hat{a}_j^1 - \hat{a}_j^2}{\hat{\sigma}^1 + \hat{\sigma}^2}$$

Since  $m_j$  should be an integer, we can choose either  $\lceil m_j^* \rceil$  or  $\lfloor m_j^* \rfloor$  whichever gives a smaller value of  $\gamma'_{x,j}$  (see Figure 6), i.e.,

$$\gamma'_{x,j} = \min \left\{ \hat{a}_j^1 - \hat{\sigma}^1 \left\lfloor \frac{\hat{a}_j^1 - \hat{a}_j^2}{\hat{\sigma}^1 + \hat{\sigma}^2} \right\rfloor, \hat{a}_j^2 + \hat{\sigma}^2 \left\lceil \frac{\hat{a}_j^1 - \hat{a}_j^2}{\hat{\sigma}^1 + \hat{\sigma}^2} \right\rceil \right\}, \forall j \in \mathcal{I}.$$

□

## A.7 Proof of Proposition 5

To prove Proposition 5, we introduce the following affine mapping defined for a subset of indices  $\mathcal{I}' \subseteq [n]$ :

$$x'_j = \begin{cases} 1 - x_j, & \forall j \in \mathcal{I}', \\ x_j, & \forall j \notin \mathcal{I}'. \end{cases}$$

This mapping can be expressed in matrix form as

$$x' = g(x) := D - Hx, \quad (\text{A.2})$$

where  $D$  is a diagonal matrix with  $D_{jj} = 1$  for  $j \in \mathcal{I}'$  and 0 otherwise, and  $H$  is a diagonal matrix with  $H_{jj} = 1$  for  $j \in \mathcal{I}'$  and  $-1$  otherwise. Since  $H^{-1} = H$ , the transformation is bijective.

**Lemma A-1.** *Let  $\mathcal{Q} = \text{conv}(\mathcal{Q}_1 \cup \mathcal{Q}_2)$ , where  $\mathcal{Q}_r = \{x \in \mathbb{R}^n : A^r x \geq b^r\}$  for some matrices  $A^r \in \mathbb{R}^{m \times n}$  and vectors  $b^r \in \mathbb{R}^m$  for  $r = 1, 2$ . Let  $\mathcal{Q}' := g(\mathcal{Q})$ , i.e., the image of  $\mathcal{Q}$  under the affine mapping (A.2). Suppose that an inequality  $\alpha_0 - \alpha_x^\top x \leq 0$  is valid for  $\mathcal{Q}$ , and let  $\beta = (\beta^1, \beta^2)$  be the associated Farkas multipliers, that is,  $(\alpha, \beta) \in \mathbb{R}^{n+1} \times \mathbb{R}_{\geq 0}^{2m}$  satisfies  $\alpha_x = (A^1)^\top \beta^1 = (A^2)^\top \beta^2$  and  $\alpha_0 \leq \min\{(b^1)^\top \beta^1, (b^2)^\top \beta^2\}$ . Then, an inequality  $\alpha'_0 - \alpha'_x^\top x' \leq 0$ , where*

$$\alpha'_{x,j} = \begin{cases} -\alpha_{x,j}, & \text{if } j \in \mathcal{I}', \\ \alpha_{x,j}, & \text{o.w.,} \end{cases} \quad (\text{A.3a})$$

$$\alpha'_0 = \alpha_0 - \sum_{j \in \mathcal{I}'} \alpha_{x,j}, \quad (\text{A.3b})$$

is valid for  $\mathcal{Q}'$ , and the associated Farkas multiplier  $\beta'$  for  $\mathcal{Q}'$  remains equal to  $\beta$ . Moreover,  $\alpha'_0 - \alpha'_x^\top \hat{x}' = \alpha_0 - \alpha_x^\top \hat{x}$ .

**Proof of Lemma A-1.** Let  $\mathcal{Q}'_r$  be the image of  $\mathcal{Q}_r$  under the affine mapping, i.e.,  $\mathcal{Q}'_r := g(\mathcal{Q}_r) = \{x' \in \mathbb{R}^n : \sum_{j \notin \mathcal{I}'} A_{\cdot j}^r x'_j - \sum_{j \in \mathcal{I}'} A_{\cdot j}^r x'_j \geq b^r - \sum_{j \in \mathcal{I}'} A_{\cdot j}^r\}$  for  $r = 1, 2$ . First, note that  $\mathcal{Q}' := g(\text{conv}(\mathcal{Q}_1 \cup \mathcal{Q}_2)) = \text{conv}(\mathcal{Q}'_1 \cup \mathcal{Q}'_2)$ , since any  $x \in \text{conv}(\mathcal{Q}_1 \cup \mathcal{Q}_2)$  can be written as  $x = \lambda x_1 + (1 - \lambda)x_2$  for some  $x_r \in \mathcal{Q}_r$  and  $\lambda \in [0, 1]$ , and we have  $g(x) = g(\lambda x_1 + (1 - \lambda)x_2) = \lambda g(x_1) + (1 - \lambda)g(x_2)$  by the affine nature of  $g$ . Therefore, it suffices to show that  $(\alpha', \beta') \in \mathbb{R}^{n+1} \times \mathbb{R}_{\geq 0}^{2m}$  defined in (A.3) satisfies

$$\alpha'_{x,j} = \begin{cases} -(A_{\cdot j}^1)^\top \beta^1 = -(A_{\cdot j}^2)^\top \beta^2, & \forall j \in \mathcal{I}', \\ (A_{\cdot j}^1)^\top \beta^1 = (A_{\cdot j}^2)^\top \beta^2, & \text{o.w.,} \end{cases} \quad (\text{A.4a})$$

$$\alpha'_0 \leq \min\{(b^1)^\top \beta^1 - \sum_{j \in \mathcal{I}'} (A_{\cdot j}^1)^\top \beta^1, (b^2)^\top \beta^2 - \sum_{j \in \mathcal{I}'} (A_{\cdot j}^2)^\top \beta^2\} \quad (\text{A.4b})$$

By setting  $\beta' = \beta$ , it is easy to see that  $\alpha'_x$  meets (A.4a). Note that  $\alpha'_0$  also satisfies (A.4b), since  $\min\{(b^1)^\top \beta^1 - \sum_{j \in \mathcal{I}'} (A_{\cdot j}^1)^\top \beta^1, (b^2)^\top \beta^2 - \sum_{j \in \mathcal{I}'} (A_{\cdot j}^2)^\top \beta^2\} = \min\{(b^1)^\top \beta^1 - \sum_{j \in \mathcal{I}'} \alpha_{x,j}, (b^2)^\top \beta^2 - \sum_{j \in \mathcal{I}'} \alpha_{x,j}\} = \min\{(b^1)^\top \beta^1, (b^2)^\top \beta^2\} - \sum_{j \in \mathcal{I}'} \alpha_{x,j} \geq \alpha_0 - \sum_{j \in \mathcal{I}'} \alpha_{x,j} = \alpha'_0$ .

It is easy to check  $\alpha'_0 - \alpha'_x^\top \hat{x}' = \alpha_0 - \alpha_x^\top \hat{x}$  since

$$\begin{aligned} \alpha'_0 - \alpha'_x^\top \hat{x}' &= \alpha_0 - \sum_{j \in \mathcal{I}'} \alpha_{x,j} + \sum_{j \in \mathcal{I}'} \alpha_{x,j} (1 - \hat{x}_j) - \sum_{j \notin \mathcal{I}'} \alpha_{x,j} \hat{x}_j \\ &= \alpha_0 - \alpha_x^\top \hat{x}. \end{aligned}$$

□

Using Lemma A-1, we now prove Proposition 5:

**Proof of Proposition 5.**

From Lemma A-1, the following will define a valid inequality  $\gamma'_0 - \gamma'_x^\top x' - \gamma'_t t' \leq 0$  for  $\mathcal{P}'_{i,n} := g(\mathcal{P}_{i,n})$ , i.e., the image of  $\mathcal{P}_{i,n}$  under the mapping  $g$  defined in (A.2) with  $\mathcal{I}' = \mathcal{I}_{n,1}$ :

$$\gamma'_{x,j} = \begin{cases} \gamma_{x,j}, & \forall j \notin \mathcal{I}_{n,1}, \\ -\gamma_{x,j}, & \forall j \in \mathcal{I}_{n,1} \end{cases}$$

and  $\gamma'_t = \gamma_t$ ,  $\gamma'_0 = \gamma_0 - \sum_{j \in \mathcal{I}_{n,1}} \gamma_{x,j}$ ,  $(\chi', \xi', \zeta') = (\chi^r, \xi^r, \zeta^r)$  for  $r = 1, 2$ .

The inequality  $\gamma'_0 - \gamma'_x^\top x' - \gamma'_t t' \leq 0$  can be lifted as  $\widehat{\gamma}'_0 - (\widehat{\gamma}'_x)^\top x' - \widehat{\gamma}'_t t' \leq 0$  that is valid for  $\mathcal{P}'_i := g(\mathcal{P}_i)$  by removing the impact of the Farkas multipliers  $(\xi', \zeta')$  for the local constraints (3.2), as follows:

$$\widehat{\gamma}'_{x,j} = \begin{cases} \gamma'_{x,j} = \gamma_{x,j}, & \forall j \notin \mathcal{I}_n, \\ \max\{\gamma'_{x,j} + \zeta_j^{1'}, \gamma'_{x,j} + \zeta_j^{2'}\} = \gamma_{x,j} + \max\{\zeta_j^1, \zeta_j^2\}, & \forall j \in \mathcal{I}_{n,0} \\ \max\{\gamma'_{x,j} + \xi_j^{1'}, \gamma'_{x,j} + \xi_j^{2'}\} = -\gamma_{x,j} + \max\{\xi_j^1, \xi_j^2\}, & \forall j \in \mathcal{I}_{n,1} \end{cases}$$

and  $\widehat{\gamma}'_t = \gamma'_t$  and  $\widehat{\gamma}'_0 = \gamma'_0$ .

Finally, using the property  $g(g(x)) = x$ , we obtain a lifted cut for  $\mathcal{P}_i$  by transforming  $\widehat{\gamma}'_0 - (\widehat{\gamma}'_x)^\top x' - \widehat{\gamma}'_t t' \leq 0$  back to  $\mathcal{P}_i = g(g(\mathcal{P}_i)) = g(\mathcal{P}'_i)$  using Lemma A-1:

$$\widehat{\gamma}'_{x,j} = \begin{cases} \widehat{\gamma}'_{x,j} = \gamma_{x,j}, & \forall j \notin \mathcal{I}_n, \\ \widehat{\gamma}'_{x,j} = \gamma_{x,j} + \max\{\zeta_j^1, \zeta_j^2\}, & \forall j \in \mathcal{I}_{n,0}, \\ -\widehat{\gamma}'_{x,j} = \gamma_{x,j} - \max\{\xi_j^1, \xi_j^2\}, & \forall j \in \mathcal{I}_{n,1}, \end{cases}$$

and  $\widehat{\gamma}_0 = \widehat{\gamma}'_0 - \sum_{j \in \mathcal{I}_{n,1}} \widehat{\gamma}'_{x,j} = \gamma'_0 + \sum_{j \in \mathcal{I}_{n,1}} (\gamma_{x,j} - \max\{\xi_j^1, \xi_j^2\}) = \gamma_0 - \sum_{j \in \mathcal{I}_{n,1}} \gamma_{x,j} + \sum_{j \in \mathcal{I}_{n,1}} (\gamma_{x,j} - \max\{\xi_j^1, \xi_j^2\}) = \gamma_0 - \sum_{j \in \mathcal{I}_{n,1}} \max\{\xi_j^1, \xi_j^2\}$ . Moreover, we have  $\widehat{\gamma}_0 - \widehat{\gamma}_x^\top \hat{x} - \widehat{\gamma}_t \hat{t} = \gamma_0 - \gamma_x^\top \hat{x} - \gamma_t \hat{t} > 0$ .

We can verify the validity of  $\widehat{\gamma}$  directly by checking whether it satisfies (2.1). To do so, we express  $\mathcal{P}_{i,n}$  and  $\mathcal{P}_i$  as follows, using some appropriate matrices and vectors  $A^r, b^r, e$ :

$\mathcal{P}_{i,n} :$

$$\begin{array}{lll} (\chi^1) \quad A^1 x + e t \geq b^1 & (\chi^2) \quad A^2 x + e t \geq b^2, & \mathcal{P}_i : \\ (\xi_j^1) \quad x_j \geq 1, \forall j \in \mathcal{I}_{n,1} & (\xi_j^2) \quad x_j \geq 1, \forall j \in \mathcal{I}_{n,1} & (\chi^1) \quad A^1 x + e t \geq b^1 \quad (\chi^2) \quad A^2 x + e t \geq b^2, \\ (\zeta_j^1) \quad -x_j \geq 0, \forall j \in \mathcal{I}_{n,0} & (\zeta_j^2) \quad -x_j \geq 0, \forall j \in \mathcal{I}_{n,0} & (\delta_j^1) \quad x_j \geq 0, \forall j \in \mathcal{I} \quad (\delta_j^2) \quad x_j \geq 0, \forall j \in \mathcal{I} \\ (\delta_j^1) \quad x_j \geq 0, \forall j \in \mathcal{I} & (\delta_j^2) \quad x_j \geq 0, \forall j \in \mathcal{I} & (\eta_j^1) \quad -x_j \geq -1, \forall j \in \mathcal{I} \quad (\eta_j^2) \quad -x_j \geq -1, \forall j \in \mathcal{I} \\ (\eta_j^1) \quad -x_j \geq -1, \forall j \in \mathcal{I} & (\eta_j^2) \quad -x_j \geq -1, \forall j \in \mathcal{I} & \end{array}$$

The characterization of valid inequalities for  $\mathcal{P}_{i,n}$  and  $\mathcal{P}_i$  are as follows [3, Theorem 1.2]:

$$\begin{aligned}
\gamma_t &= e^\top \chi^1 = e^\top \chi^2, & \gamma_t &= e^\top \chi^1 = e^\top \chi^2, \\
\gamma_{x,j} &= (A_{\cdot j}^1)^\top \chi^1 = (A_{\cdot j}^2)^\top \chi^2, \forall j \in [n_x] \setminus \mathcal{I}, & \gamma_{x,j} &= (A_{\cdot j}^1)^\top \chi^1 = (A_{\cdot j}^2)^\top \chi^2, \forall j \in [n_x] \setminus \mathcal{I}, \\
\gamma_{x,j} &= (A_{\cdot j}^1)^\top \chi^1 + \delta_j^1 - \eta_j^1 & \gamma_{x,j} &= (A_{\cdot j}^1)^\top \chi^1 + \delta_j^1 - \eta_j^1 \\
&= (A_{\cdot j}^2)^\top \chi^2 + \delta_j^2 - \eta_j^2, \forall j \in \mathcal{I} \setminus \mathcal{I}_{n,0} \cup \mathcal{I}_{n,1}, & &= (A_{\cdot j}^2)^\top \chi^2 + \delta_j^2 - \eta_j^2, \forall j \in \mathcal{I} \setminus \mathcal{I}_{n,0} \cup \mathcal{I}_{n,1}, \\
\gamma_{x,j} &= (A_{\cdot j}^1)^\top \chi^1 + \delta_j^1 - \eta_j^1 - \zeta_j^1 & \gamma_{x,j} &= (A_{\cdot j}^1)^\top \chi^1 + \delta_j^1 - \eta_j^1 \\
&= (A_{\cdot j}^2)^\top \chi^2 + \delta_j^2 - \eta_j^2 - \zeta_j^2, \forall j \in \mathcal{I}_{n,0}, & &= (A_{\cdot j}^2)^\top \chi^2 + \delta_j^2 - \eta_j^2, \forall j \in \mathcal{I}_{n,0}, \\
\gamma_{x,j} &= (A_{\cdot j}^1)^\top \chi^1 + \delta_j^1 - \eta_j^1 + \xi_j^1 & \gamma_{x,j} &= (A_{\cdot j}^1)^\top \chi^1 + \delta_j^1 - \eta_j^1 \\
&= (A_{\cdot j}^2)^\top \chi^2 + \delta_j^2 - \eta_j^2 + \xi_j^2, \forall j \in \mathcal{I}_{n,1}, & &= (A_{\cdot j}^2)^\top \chi^2 + \delta_j^2 - \eta_j^2, \forall j \in \mathcal{I}_{n,1}, \\
\gamma_0 &\leq (b^1)^\top \chi^1 - \sum_{j \in \mathcal{I}} \eta_j^1 + \sum_{j \in \mathcal{I}_{n,1}} \xi_j^1, & \gamma_0 &\leq (b^1)^\top \chi^1 - \sum_{j \in \mathcal{I}} \eta_j^1, \\
\gamma_0 &\leq (b^2)^\top \chi^2 - \sum_{j \in \mathcal{I}} \eta_j^2 + \sum_{j \in \mathcal{I}_{n,1}} \xi_j^2. & \gamma_0 &\leq (b^2)^\top \chi^2 - \sum_{j \in \mathcal{I}} \eta_j^2,
\end{aligned}$$

Thus,  $(\gamma, \chi, \zeta, \xi)$  satisfies the system on the left. Consequently, the modification in (3.3) results in:

$$\begin{aligned}
\gamma_t &= e^\top \chi^1 = e^\top \chi^2, \\
\gamma_{x,j} &= (A_{\cdot j}^1)^\top \chi^1 = (A_{\cdot j}^2)^\top \chi^2, \forall j \in [n_x] \setminus \mathcal{I}, \\
\gamma_{x,j} &= (A_{\cdot j}^1)^\top \chi^1 + \delta_j^1 - \eta_j^1 \\
&= (A_{\cdot j}^2)^\top \chi^2 + \delta_j^2 - \eta_j^2, \forall j \in \mathcal{I} \setminus \mathcal{I}_{n,0} \cup \mathcal{I}_{n,1}, \\
\hat{\gamma}_{x,j} &= (A_{\cdot j}^1)^\top \chi^1 + \delta_j^1 - \eta_j^1 - \zeta_j^1 + \max\{\zeta_j^1, \zeta_j^2\} \\
&= (A_{\cdot j}^2)^\top \chi^2 + \delta_j^2 - \eta_j^2 - \zeta_j^2 + \max\{\zeta_j^1, \zeta_j^2\}, \forall j \in \mathcal{I}_{n,0}, \\
\hat{\gamma}_{x,j} &= (A_{\cdot j}^1)^\top \chi^1 + \delta_j^1 - \eta_j^1 + \xi_j^1 - \max\{\xi_j^1, \xi_j^2\} \\
&= (A_{\cdot j}^2)^\top \chi^2 + \delta_j^2 - \eta_j^2 + \xi_j^2 - \max\{\xi_j^1, \xi_j^2\}, \forall j \in \mathcal{I}_{n,1}, \\
\hat{\gamma}_0 &\leq (b^1)^\top \chi^1 - \sum_{j \in \mathcal{I}} \eta_j^1 + \sum_{j \in \mathcal{I}_{n,1}} (\xi_j^1 - \max\{\xi_j^1, \xi_j^2\}), \\
\hat{\gamma}_0 &\leq (b^2)^\top \chi^2 - \sum_{j \in \mathcal{I}} \eta_j^2 + \sum_{j \in \mathcal{I}_{n,1}} (\xi_j^2 - \max\{\xi_j^1, \xi_j^2\}),
\end{aligned}$$

which clearly show that  $\hat{\gamma}$ , together with  $\hat{\chi}$  in (3.4), satisfies the valid inequality characterization for  $\mathcal{P}_i$ .  $\square$

## A.8 Proof of Theorem 2

Upon full convergence of the while loop in Line 4,  $(\tau, \gamma)$  is an optimal solution to  $(\text{DCGLP}_{\mathcal{I}})$  where  $(\text{DCGLP}_{\mathcal{I}})$  is a restriction of  $(\text{DCGLP})$  incorporating the additional constraints from Line 3. Therefore,  $\tau \geq v_{(\text{DCGLP})} = v_{(\text{CGLP})}$ . From Proposition 5, we have  $\hat{\gamma} \in \Gamma$ , where  $\Gamma$  is the feasible region of  $(\text{CGLP})$  without the normalization constraint, i.e., (2.1). Since  $\Gamma$  is conic,  $\hat{\gamma}$  can be made feasible to  $(\text{CGLP})$  by normalizing it with a nonnegative scalar  $\frac{1}{\max\{\|(\hat{\gamma}_x, \hat{\gamma}_t)\|_q, 1\}}$ . The resultant feasible solution evaluates the objective function of  $(\text{CGLP})$  at  $\frac{\tau}{\max\{\|(\hat{\gamma}_x, \hat{\gamma}_t)\|_q, 1\}}$ , and thus  $v_{(\text{CGLP})} \geq \frac{\tau}{\max\{\|(\hat{\gamma}_x, \hat{\gamma}_t)\|_q, 1\}}$ .  $\square$

## Appendix B Formulation of benchmark problems

### B.1 Uncapacitated Facility Location Problem

The Uncapacitated Facility Location Problem (UFLP) is formulated as a MILP to minimize total costs, including facility opening costs and transportation costs. Given  $I$  as the total number of potential facility locations and  $J$  as the total number of customer nodes, let  $c_{i,j}$  be the transportation cost from facility  $i$  to customer  $j$ . Binary variables  $x_i$  indicate whether facility  $i$  is opened, and continuous variables  $y_{i,j}$  represent the fraction of customer  $j$ 's demand satisfied by facility  $i$ . The classical UFLP model is expressed as follows:

$$\begin{aligned} \min_{x,y} \quad & \sum_{i \in [I]} f_i x_i + \sum_{i \in [I]} \sum_{j \in [J]} c_{i,j} y_{i,j} \\ \text{s.t.} \quad & \sum_{i \in [I]} y_{i,j} = 1, \quad \forall j \in [J] \\ & y_{i,j} \leq x_i, \quad \forall i \in [I], j \in [J] \\ & x_i \in \{0, 1\}, \quad y_{i,j} \geq 0, \quad \forall i \in [I], j \in [J] \end{aligned}$$

Since the UFLP has no coupling constraint, the subproblem becomes separable with respect to each customer  $j$ . In addition to the classical UFLP model, we consider  $\sum_{i \in [I]} x_i \geq 2$  in the master problem of the BD. Since we can easily compute the optimal objective value for the case when  $\sum_{i \in [I]} x_i = 1$ , we excluded it from the framework as proposed by [16].

### B.2 Stochastic Network Interdiction Problem

The Stochastic Network Interdiction Problem (SNIP) aims to minimize the expected probability of an intruder reaching the destination across scenarios by deploying sensors on eligible arcs. Let  $N$  denote the total number of nodes and  $A$  set of arcs, with  $D \subseteq A$  as the subset of arcs where sensors can be placed. Let  $K$  denote the total number of scenarios. In the first-stage problem, given a budget  $b$ , the interdictor places sensors on arcs, knowing a priori probability of an intruder avoiding detection with and without a sensor on arc  $(i, j)$  denoted as  $r_{i,j}$  and  $q_{i,j}$  respectively. The interdictor makes the decision without knowing the origin ( $o_k$ ) and the destination ( $d_k$ ) of the intruder for each scenario  $k \in [K]$ . In the second-stage problem, the intruder maximizes the likelihood of evading surveillance by selecting a maximum reliability path. When no sensors are placed,  $\psi_{j,k}$  denotes the value of a maximum reliability path from node  $j \in [N]$  to the destination  $d_k$ , computed by solving a shortest path problem [29], and is used to adjust the evasion probability based on the installation. Binary variables  $x_{i,j}$ , used in the first-stage, indicate whether a sensor is deployed on arc  $(i, j) \in D$ , while continuous variables  $y_{i,k}$ , used in the second-stage, represent the probability of the intruder traversing from node  $i \in [N]$  to destination  $d_k$  without detection. The extensive formulation of SNIP is as follows:

$$\begin{aligned}
\min_{x,y} \quad & \sum_{k \in [K]} p_k y_{o_k, k} \\
\text{s.t.} \quad & \sum_{(i,j) \in D} x_{ij} \leq b \\
& y_{d_k, k} = 1, \quad \forall k \in [K] \\
& y_{i,k} - r_{i,j} y_{j,k} \geq 0, \quad \forall (i,j) \in A \setminus D, k \in [K] \\
& y_{i,k} - r_{i,j} y_{j,k} \geq -(r_{i,j} - q_{i,j}) \psi_{j,k} x_{i,j}, \quad \forall (i,j) \in D, k \in [K] \\
& y_{i,k} - q_{i,j} y_{j,k} \geq 0, \quad \forall (i,j) \in D, k \in [K] \\
& x_{i,j} \in \{0, 1\}^{|D|}, \quad y_{i,k} \geq 0, \quad \forall i \in [N], k \in [K]
\end{aligned}$$